Dissertation zur Erlangung des Doktorgrades

der Fakultät für Chemie und Pharmazie

der Ludwig-Maximilians-Universität München

Identification and Functional Analysis of Novel HCN2 Channel Interactors

Verena Hammelmann

aus Nürnberg

2010

Erklärung

Diese Dissertation wurde im Sinne von § 13 Abs. 3 bzw. 4 der Promotionsordnung vom 29. Januar 1998 von Prof. Dr. Martin Biel betreut.

Ehrenwörtliche Versicherung

Hiermit versichere ich ehrenwörtlich, dass die vorgelegte Arbeit selbstständig und ohne unerlaubte Hilfe verfasst wurde. Es wurden keine anderen Hilfsmittel außer den angegebenen verwendet.

München, den 22.11.2010 .....

(Verena Hammelmann)

Dissertation eingereicht am 22.11.2010

1. Gutachter: Prof. Dr. Martin Biel

2. Gutachter: Prof. Dr. Christian Wahl-Schott

Mündliche Prüfung am 13. 12.2010

Table of contents

1 Introduction

1.1 The Hyperpolarization-activated Current I_h

I_h is a mixed Na^+ and K^+ cationic current (= I) which is slowly activated by hyperpolarization (= h) and facilitated by cyclic nucleotides. This unique current was first discovered in sinoatrial node cells (Brown et al. 1977, DiFrancesco 1981) and in neurons (Halliwell and Adams 1982) in the late 1970s and early 1980s. Owing to its unusual biophysical properties, I_h was also denoted "funny" (I_f) (Brown et al. 1979) and "queer" (I_q). In the following, only the term I_h will be used.

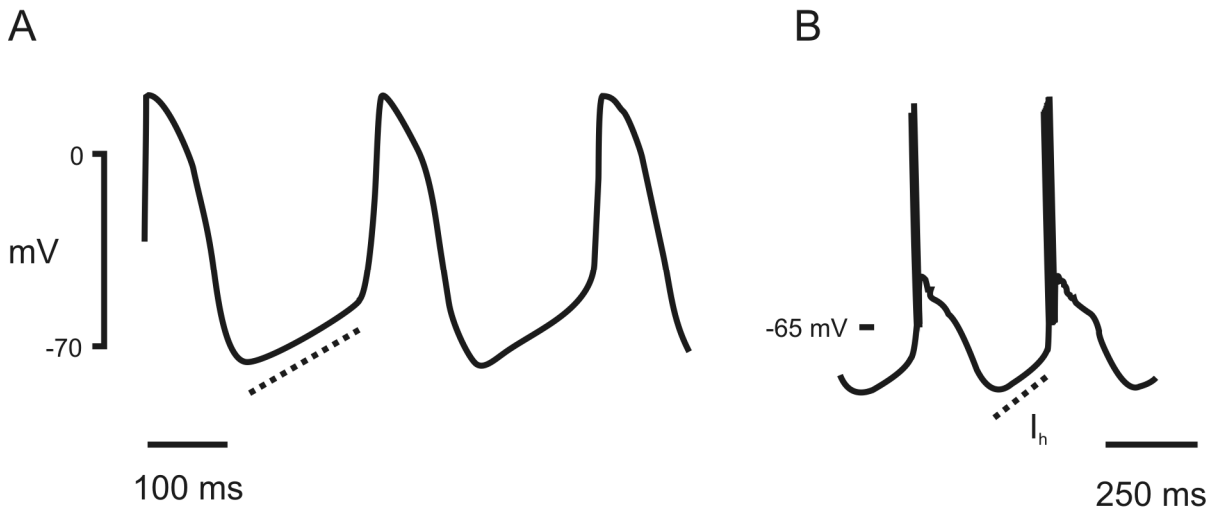

Fig. 1: Pacemaker role of I_h (A) Firing modes of thalamocortical neurons, I_h is indicated as a dashed line. **(B)** Idealised pacemaker potentials in the absence of adrenergic stimulation. DD: diastolic depolarization, time scale is indicated as a black bar. Adapted from Biel et al. 2009.

I_h is widely found in the central nervous system and in heart and has been known to play a key role in controlling neuronal and cardiac rhythmicity (Fig. 1). Sinoatrial node cells generate a pacemaker potential that is characterised by the presence of a progressive diastolic depolarization (DD) (Fig. 1A). DD results from a net inward current starting at the end of the repolarization. I_h is a major (but not the only) component contributing to the DD. In the central nervous system, I_h exists in a variety of neurons which function as pacemaker units. These pacemaker neurons control rhythmic oscillations of single neurons and neuronal networks (e.g. in the Thalamus, Fig. 1B) concerning sleep, sensory processing and seizures (McCormick and Pape 1990, Luthi and McCormick 1998).

Besides its pacemaker function, I_h contributes to other basic neuronal processes, including the determination of the resting membrane potential (Ludwig et al. 2003, Day et al. 2005, Nolan et al.

2007), dendritic integration (Magee 1998, Williams and Stuart 2000) and synaptic transmission (Beaumont and Zucker 2000).

1.2 Structure of HCN Channels

The ion channels passing I_h were first cloned in the late 90ies (Gauss et al. 1998, Ludwig et al. 1998, Santoro et al. 1998, Ludwig et al. 1999). Structurally, the four members of the **H**yperpolarization-activated **c**yclic **n**ucleotide-gated (HCN) channel family (HCN1-4) belong to the superfamily of pore-loop cation channels (Biel et al. 2009).

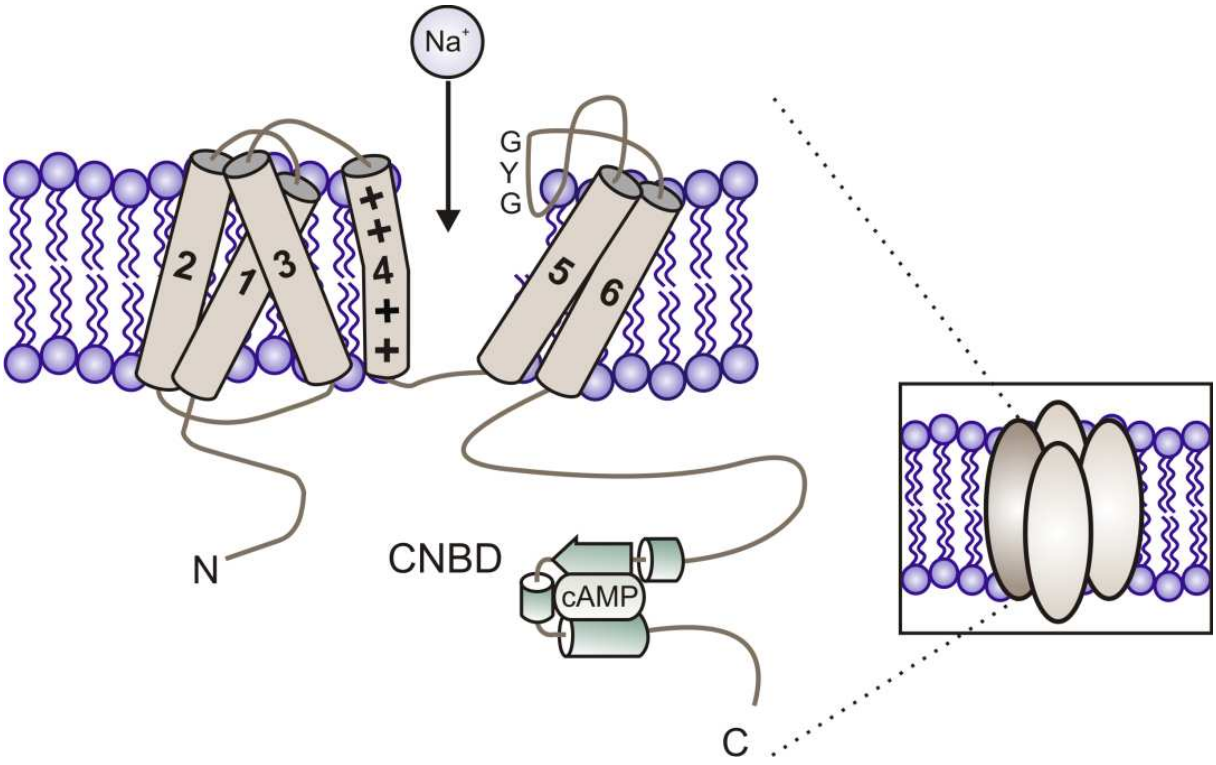

Fig. 2: Structure of HCN channels. HCN channels consist of four homologous or identical subunits (homo/heteromeric structure). Each of the four subunits comprises six transmembrane segments including the voltage sensor (S4) and the pore region between S5 and S6. The pore region carries a GYG motif as selectivity filter. N- and C-termini are located intracellulary. The C-terminal channel domain contains a cyclic nucleotide-binding domain (CNBD). Adapted from Biel et al. 2009.

HCN channels can either form homotetramers or heterotetramers of the subunits HCN1-4. Each subunit is composed of six α-helical transmembrane segments (S1-6) whereas the N- and C-termini are located intracellulary. The S4 segment carries nine arginine or lysine residues regularly spaced at every third position and represents the positively charged voltage sensor. The pore is formed by the

S6 segment and the loop. This pore forming unit is closely related to the pore of highly selective K^+ channels (Fig. 2).

HCN channel subunits contain a GYG sequence which is the hallmark for K^+ selectivity. Nevertheless, the channels conduct both K^+ and Na^+ but under physiological conditions it is the Na^+ current that is most relevant. Currently it is unknown which structural determinant confers to the permeation of Na^+ in the channel. However, it is tempting to speculate that in the tetrameric HCN channel complex the GYG motif is coordinated in a less rigid fashion than in K^+ channels, allowing the entrance of cations of different size.

The C-terminus of the HCN channel subunit contains a cyclic nucleotide-binding domain (CNBD) which is connected to the S6 segment of the transmembrane core via the C-linker. The CNBD is a highly conserved protein domain that can bind the cyclic nucleotides cAMP and cGMP. The recently published crystal structure of the mouse HCN2 C-terminal fragment including the C-linker and the CNBD provided insights into the cGMP-dependent gating in HCN channels (Zagotta et al. 2003). Nevertheless, the conformational changes during the gating process are not fully understood. The CNBD comprises an initial α-helix (A-helix), followed by an eight-stranded antiparallel β-roll (β1-β8), a short B-helix and a long C-helix. The binding pocket for cyclic nucleotides is formed by a number of residues at the interface between the β-roll and the C-helix (Fig. 2). Central role plays the interaction between the negatively charged cyclic-phosphate group in cyclic nucleotides and a positively charged arginine residue (R591 in the HCN2 subunit) which has been shown to be crucial on both CNG and HCN channels (Tibbs et al. 1998).

1.3 Modulation by Cyclic Nucleotides

Although all four HCN family members share a highly conserved CNBD, the response to cyclic nucleotides is quite different.

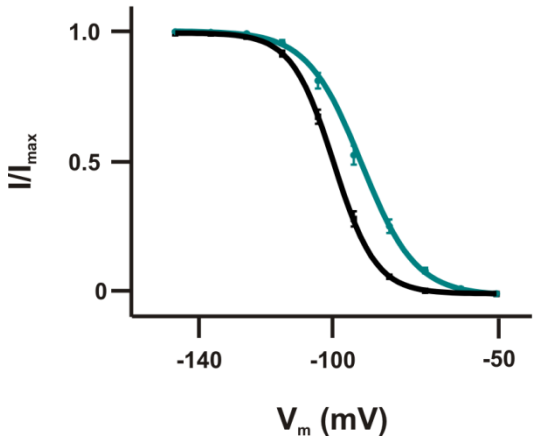

Fig. 3: Activation curve of I_h of HCN2 stable transfected HEK 293 cells in absence (black) or presence (blue) of cyclic nucleotides. Cyclic nucleotides shift the activation curve of I_h to more positive potentials.

The activation curves of HCN2 and HCN4 are shifted by about +10 to +25 mV to more positive voltages when cyclic nucleotides are added (Fig. 3) and the channel opening is accelerated (DiFrancesco and Tortora 1991). In contrast, HCN1 and HCN3 are, if at all, only weakly affected by cyclic nucleotides (Santoro et al. 1998, Mistrik et al. 2005, Stieber et al. 2005). While the extent of the shift is similar for both, cAMP and cGMP, the affinities are 10 to 100-fold higher for cAMP (K_a = 60-500 nM) than for cGMP (K_a = 6 µM) (Ludwig et al. 1998). Several residues in the C-helix contribute to the higher selectivity of HCN channels for cAMP than for cGMP (Zhou and Siegelbaum 2007).

The channel cannot be opened by cyclic nucleotides alone without additional hyperpolarization. The phenomenon that the HCN channel is activated by hyperpolarization and that the voltage-dependence of activation is speed up by cyclic nucleotides is termed *dual gating*. The activation of HCN channels is thus a combined process which consists of a voltage- and a ligand (cyclic nucleotide) component.

1.4 Regulation of HCN Channels

HCN channels are tightly regulated by interacting proteins as well as by low molecular factors in the cytosol and the extracellular space. These molecules control the functional properties of the channels in the plasma membrane and influence their targeting to cellular compartments or regulate their surface expression. Fig. 4 gives an overview on known interacting proteins and low molecular factors that modulate the HCN channels.

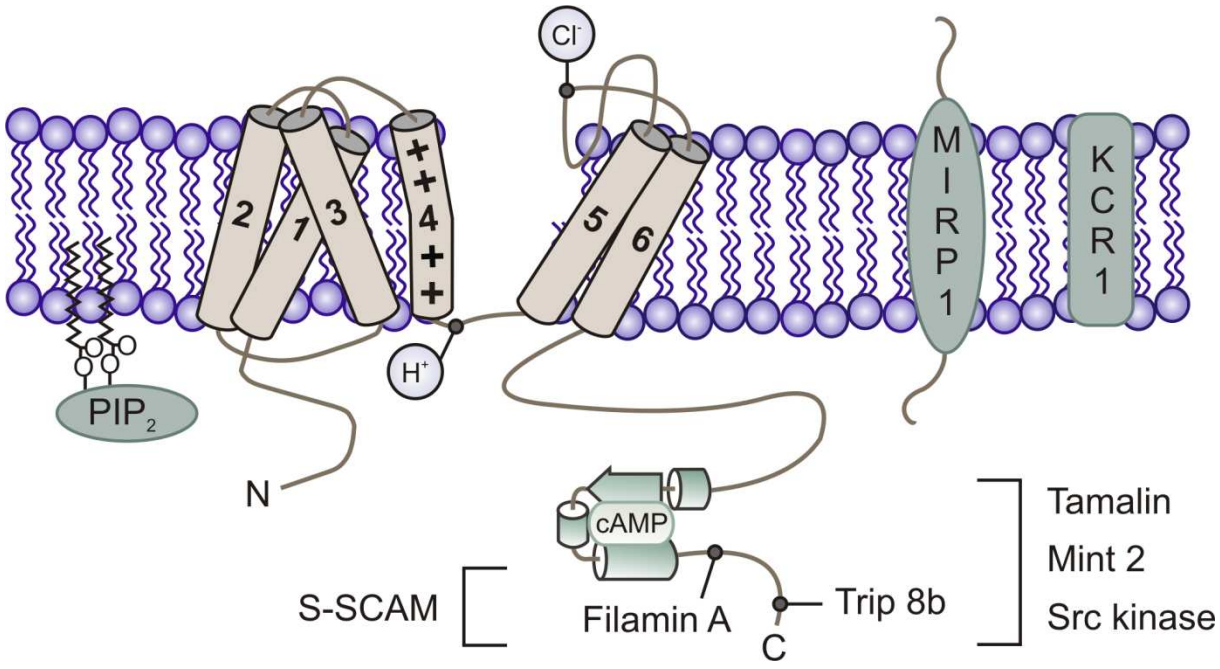

Fig. 4: Regulation of HCN channels by interacting proteins and low molecular factors. cAMP, Cl^-, Filamin A, H^+, KCR1, Mint2, MiRP1, PIP_2, Src kinase, S-SCAM, Tamalin and Trip8b interact with the HCN channel in distinct regions, here shown for one HCN channel subunit. Adapted from Biel et al. 2009.

1.4.1 Modulation by Low Molecular Factors

1.4.1.1 Regulation by PIP_2

In excised patches, heterologously expressed HCN channel currents display a rapid rundown which becomes apparent in an about 30-50 mV hyperpolarizing shift of the activation curve. The washout of cyclic nucleotides can only partially explain the hyperpolarizing shift. The missing factor for the rundown was recently identified as PIP_2 (Pian et al. 2006, Zolles et al. 2006). Studies gave strong evidence that HCN channels are regulated by phosphatidylinositol 4, 5-bisphosphate (PIP_2), like a number of other ion channels as well (for review, see Gamper and Shapiro 2007, Suh and Hille 2008). In HCN channels, PIP_2 acts as an allosteric activator which leads to a positive shift of $V_{0.5}$ by about 20 mV to more positive potentials in a cyclic nucleotide independent manner (Pian et al. 2006, Zolles et al. 2006). Thus, together with the depolarizing shift of cyclic nucleotides, the influence of PIP_2 enables robust channel activation in the voltage range relevant for the physiological role of HCN channels.

1.4.1.2 Regulation by Protons

HCN channels are regulated by external and internal protons. There is evidence that the $V_{0.5}$ is a function of the proton concentration (Zong et al. 2001). Intracellulary, a histidine residue was

identified which controls the pH-dependent change in the $V_{0.5}$ (Fig. 4). The physiological role of the pH modulation of HCN channels may have influence on sleep spindle oscillations or the respiratory frequency (Munsch and Pape 1999).

Extracellular pH changes can also influence the HCN channel activity. A low extracellular pH value strongly activates HCN1 and HCN4 channels, respectively in rat taste cells, suggesting that HCN channels may function as additional receptors for sour taste (Stevens et al. 2001). The underlying mechanism and the relevance of the regulation by external pH are not yet determined.

1.4.1.3 Regulation by Chloride

Anions do have an influence on channel activity, although HCN channels do not conduct anions. The replacement of chloride for bulkier anions like glutamate, acetate, and aspartate decreased the amplitude of I_h in rabbit sinoatrial node cells (Frace et al. 1992). A single arginine residue in the pore region of HCN2 and HCN4 channels seems to be responsible for the chloride sensitivity. HCN1 and HCN3 lack this arginine residue and exhibit the response to chloride (Fig. 4) (Wahl-Schott et al. 2005). A reduction of I_h in sinoatrial cells may be involved in the generation of arrhythmias observed in hypochloremias.

1.4.2 Regulation by Accessory Proteins

There is growing evidence that ion channels form macromolecular complexes with membrane spanning and cytosolic proteins (Muller et al. 2010). The trafficking and function of many ion channels are regulated by subunits that do not contribute to the pore-forming core of the channel.

1.4.2.1 Regulation by MiRP-1

The HCN1 and HCN2 current amplitude is increased in heterologous expression systems when co-transfected with MiRP-1 and the current expression is enhanced (Yu et al. 2001, Qu et al. 2004). Whereas MiRP-1 can accelerate the HCN1 and HCN2 activation and deactivation kinetics, the activation rate of HCN4 channel is slowed down (Decher et al. 2003). MiRP-1 is a member of single transmembrane-spanning proteins and serves as an auxiliary subunit of the HERG delayed rectifier K^+ channels. The C-Terminus of MiRP-1 interacts with the C-terminus of HCN2 and HCN4 (Fig. 4) (Decher et al. 2003). However, all data supporting a functional role for MiRP-1 on HCN channels were obtained in heterologous expression systems. Therefore, it will be necessary to verify the interaction between MiRP-1 and the HCN subunits together with its functional implications in native tissues.

1.4.2.2 Regulation by KCR1

Recently, another transmembrane-associated protein was reported to interact with the HCN2 channel (Fig. 4). The K^+ channel regulator 1 consists of 12 putative transmembrane segments. The loss of KCR1 function results in an increase of I_h current density. In the same study it was shown that viral overexpression in rat cardiomyocytes also reduced the current density of native I_h and suppressed the spontaneous action potential activity of these channels (Michels et al. 2008).

1.4.2.3 Regulation by Scaffold Proteins

Scaffold proteins like TPR-containing Rab8b interacting protein (Trip8b) (Santoro et al. 2004), Tamalin, S-SCAM and Mint2 (Kimura et al. 2004) were reported to affect HCN channel trafficking and, thus, I_h current density.

Trip8b was found in a proteomic approach (Zolles et al. 2009) and is potentially the major endogenous auxiliary subunit of HCN channels in the mammalian brain. Nine alternative N-terminal splice isoforms of the brain specific Trip8b protein have been identified. When co-expressed with HCN1 in HEK 293 cells or hippocampal neurons, these variants differentially up- or downregulated I_h (Santoro et al. 2009, Zolles et al. 2009). These effects were mediated by alterations in the HCN channel surface expression resulting from a change in HCN subunit trafficking (Santoro et al. 2009, Zolles et al. 2009). Regardless of the Trip8b isoform tested, the membrane potential threshold for HCN channel activation was shifted to more hyperpolarized potentials (Lewis et al. 2009, Santoro et al. 2009). Moreover, Trip8b also altered HCN channel gating by slowing the channel opening and accelerating the channel closing (Santoro et al. 2009, Zolles et al. 2009).

Additionally, the HCN2 channel forms a protein assembly with the neuronal scaffold proteins Tamalin, S-SCAM and Mint2 via distinct protein binding domains in the C-terminus. In overexpressed systems, the HCN2 surface expression was increased upon co-expression with Mint2 suggesting that this protein might be a positive regulator of cell surface expression of HCN channels (Kimura et al. 2004).

1.4.2.4 Regulation by Filamin A

On the basis of overexpression systems, Filamin A is suggested to cause a clustering of HCN1 channels, thereby slowing down the channel activation and deactivation (Gravante et al. 2004).

Filamin A is a putative cytoplasmatic scaffold protein and binds to HCN1 via a 22 amino acid region downstream the CNBD.

1.4.3 Regulation by Protein Modification

Posttranslational modification is a common feature of proteins. During this process, the modification by phosphorylation is a major mechanism involved in the modulation of ion channel properties and function.

1.4.3.1 Regulation by Src Kinase

Pharmacological blocking experiments showed that I_h is regulated by tyrosine kinases of the Src family (Wu and Cohen 1997). This hypothesis was confirmed by yeast two hybrid screens that proofed an interaction between Src and the HCN1 channel as well as Src and HCN2 (Santoro et al. 1997, Zong et al. 2005). The direct binding of Src to HCN2 and HCN4 could be verified in co-immunoprecipitation experiments in heterologous expression systems and in native tissue (Zong et al. 2005, Arinsburg et al. 2006). Yeast two hybrid experiments showed that the SH3 domain of Src binds to the C-linker-CNBD domain of HCN2 and phosphorylates the channel at this domain (Zong et al. 2005). As a consequence of the phosphorylation, the activation kinetics of the channel is accelerated. An inhibition of Src kinases led to a slow-down of the HCN2 current corresponding to an increase in the activation time constant. The HCN2 channel is phosphorylated by the Src kinase at a tyrosine residue at position 476 in a region which is highly conserved among HCN1-4 subunits. The substitution of this amino acid by phenylalanine in either HCN2 or HCN4 led to channel mutants that were not longer modulated by the Src kinase. Another tyrosine residue was found recently in HCN4 channels at position 531 that may be involved in Src mediated channel regulation (Li et al. 2008). The additional phosphorylation not only speeds up channel kinetic but also shifted the voltage-dependence of activation to more positive potentials and led to the increase of the whole cell channel conductance (Li et al. 2008). Taken together, the results indicate that the control of the phosphorylation status is indeed an important regulatory mechanism to adjust the properties I_h to the specific requirements of different cell types of neurons and heart cells.

1.4.3.2 Regulation by p38 Mitogen Activated Protein Kinase (p38 MAPK)

The p38 MAPK interacts with the HCN1 and HCN2 in CA1 pyramidal neuron dendrites and pyramidal-like principal neuron somata (Poolos et al. 2006). Pharmacological blockade of p38 MAPK activity

significantly downregulated I_h in hippocampal neurons, with a 25 mV hyperpolarizing shift in voltage-dependent activation. Consequently, the neuronal resting membrane potential was shifted to more hyperpolarized potentials and the neuronal input resistance was increased as well as the temporal summation. Lately, it was discovered that during epileptogenesis in the pilocarpine model of epilepsy, HCN channels underwent a progressive downregulation of their voltage-dependent gating and act in concert with the gradual increase in seizure frequency (Jung et al. 2007). This downregulation was found to be mediated at least by the persistent alteration of two distinct phosphorylation pathways. Firstly, a reduced p38 MAPK activity in hippocampal area CA1 from chronically epileptic animals and, secondly, an enhanced activity of the phosphatase calcineurin which consequently produces neuronal hyperexcitability (Jung et al. 2010). It remains unclear whether p38 MAPK directly phosphorylates the HCN channel. Since the phosphorylation sites on the HCN channel were not mapped so far, it is also likely that HCN channel gating is modulated by other kinases and phosphatases or via phospholipids pathways.

1.4.3.3 Regulation by Protein Kinase A (PKA)

The cAMP-dependent protein kinase A (PKA) is the major target for cAMP action in eukaryotic cells. It was speculated for a long time that there is a link between HCN channels and their modulation by cyclic nucleotides via the PKA. HCN channels contain numerous consensus PKA phosphorylation sites and the inhibition of PKA shifted the half-maximal activation voltage to more negative potentials in purkinje fibres (Chang et al. 1991) and in cultured rat olfactory receptor neurons (Vargas and Lucero 2002). In isolated ventricular myocytes, I_h phosphorylation also produces a positive shift in the I_h activation curve, but it was not clear whether the conductance was regulated as well (Yu et al. 1995). Recently, it was reported that PKA might directly phosphorylate the HCN4 channel at various sites in the N- and C-termini (Liao et al. 2010). As a consequence, phosphorylation of the HCN4 channel via PKA shifted the voltage-dependence of activation by 6 mV to more positive potentials in sinoatrial myocytes as well as in heterologous expression systems. The phosphorylation by PKA is discussed controversial. One reason is that direct phosphorylation could not be proofed in mammalian cells or native tissue. Moreover, it seems implausible that the PKA is postulated to phosphorylate at least 13 residues within the HCN4 channel. According to the current state of knowledge, the PKA seems to have an influence in I_h. The importance of the PKA-mediated regulation has to be considered critically and remains to be determined.

1.5 Aim of this Study

HCN channels are key regulators of cellular excitability in the heart and the nervous system. Previous work indicated that the activity of HCN channels is tightly regulated by low-molecular cellular factors (e.g. protons, Cl^-, PIP_2) as well as by protein phosphorylation. There is also growing evidence that HCN channels do not exist in isolation in the plasma membrane but are rather part of multi-protein complex whose composition is cell type-specific and dynamically regulated by the cell.

In order to achieve a deeper understanding of the cellular role of HCN channels it is crucial to determine the individual components of the HCN channel signalling complex. The present study was launched to experimentally address this important issue. In a first approach, an unbiased yeast-two hybrid screen should be performed with cDNA from mouse brain to identify proteins that interact with HCN channels in neurons. A particular focus should be on proteins that interact with the large intracellular C-terminus of HCN2, the channel subunit which is the most wide-spread member of the HCN channel family. As a first step into functional analysis the identified HCN2 interacting proteins should be validated biochemically using GST-pulldown assays, co-immunoprecipitation and immunocytochemistry. In the second part of the study the potential regulation of HCN2 by the cGMP-dependent protein kinase should be investigated. The rationale behind this approach was the idea that cGMP -like cAMP- may regulate channel activity via two different pathways, namely by (1) direct interaction with the CNBD and (2) by mediating channel phosphorylation. To examine the validity of this hypothesis an array of biochemical and electrophysiological methods should be employed. These experiments should be complemented by experiments with tissues from genetic mouse models lacking either HCN2 or PKGs.

2 Materials and Methods

2.1 Chemicals, Solutions and Buffers

All chemicals used were obtained by Merck, Roth, Sigma-Aldrich and Bio-Rad if not mentioned extraordinarily. The quality was “pro analysi” or “for molecular biological use”. For all solutions high pure and deionised water was used (high pure water system Easypure UV/UF, Werner GmbH). In experiments in which a high purity was required all solutions were autoclaved.

2.2 Plasmids

Plasmids are circular double-stranded DNA molecules which have their origin in bacteria. They are located extrachromosomally and are replicated autonomously. For the molecular use, these plasmids are modified in order to amplify DNA or to subsequently express proteins. Essentials of so called expression vectors are the *origin of replication*, a resistance gene encoding for an antibiotic used for selection and a *multiple cloning site (MCS)*. In this polylinker, various recognition sites for restriction endonucleases are placed allowing cloning of DNA fragments.

pcDNA3 (5.4 kb) and **pcDNA3.1** (5.5 kb, Invitrogen)

Characteristic elements of these eukaryotic expression vectors are a cytomegalovirus-promoter (CMV-promoter) which enables a strong and constitutive expression and a resistance gene encoding for ampicillin. The difference between the pcDNA3 and the pcDNA3.1 vector is the presence of a carboxy-teminal myc-tag in the reading frame of pcDNA3.1 which allows easy detection and immunoprecipitation of proteins. In this work, the pcDNA3 and pcDNA3.1 vectors were used for heterologous expression of HCN subunits and corresponding interactors in various protein studies.

pCRII-TOPO® (3.9 kb, Invitrogen)

This vector was used for cloning of PCR products (see chapter 2.4.8). It contains a lacZ promoter followed by the MCS and lacZ reporter gene. Thus, insertion of constructs into the MCS disrupts the expression of β-galactosidase and can be used for selection of recombinant bacterial clones on X-gal containing plates. Additionally, this vector contains a f1 ori and pUC ori for plasmid replication in prokaryotes. For selection of recombinant bacteria, kanamycin and ampicillin resistance (Amp^R) are included in this vector.

pIRES-EGFP (5.3 kb, Clonetech)

This bicistronic vector carries besides a CMV-promoter, a resistance gene for kanamycin and a sequence for the *internal ribosome entry site* (IRES-sequence). Its location between the MCS and a coding sequence for the *enhanced green fluorescent protein* (eGFP) allows simultaneous expression of two independent proteins. In patch clamp experiments transfected cells could easily be detected by green fluorescence.

pMyr (5.6 kb, Stratagene)

The pMyr vector is used as a component of the CytoTrap two-hybrid system and express proteins fused to a myristylation signal. In this study, the pMyr vector contained the target proteins from the brain cDNA-library. Owing to the myristylation signal, proteins expressed from this vector are directed to the cytoplasmatic part of the cell membrane. The pMyr vector exhibits various features for protein expression in yeast: expression of the myristylated target protein starting with the GAL1 promoter which is repressed when yeast are grown in the presence of glucose but depressed in the presence of galactose. For selection in yeast, a URA3 gene is included which allows growth on uracile deficient agar plates. The chloramphenicol-resistance gene conduces to selection in *E.coli*.

pSOS (11.3 kb, Stratagene)

The pSOS vector is the second component of the CytoTrap two-hybrid system (Y2H). DNA encoding the protein of interest (bait protein) is cloned into the pSos vector MCS, generating a fusion protein of hSos and the bait protein. In this Y2H screen, the C-terminus of the HCN2 subunit was cloned in pSOS. The *ADH1* promoter driving expression of the hSos-bait fusion is constitutively active. A LEU2 gene allows endogenous leucine production to grow on leucine deficient agar plates. For selection in *E.coli*, an ampicillin-resistance gene is included.

pET41a (6.0 kb, Novagen)

The pET41a vector was used to fuse a N-terminal schistosomal glutathione-S-transferase tag to the protein of interest (GST-tag) which is driven by the T7 *lac* promoter The protein expression can be induced by Isopropyl-β-D-thiogalactopyranosid (IPTG) since it inactivates the *lac*Z repressor and, therefore, induces transcription of the *lac* operon. A kanamycin resistance gene allows selection.

pQE30 (3.5 kb, Quiagen)

The pQE is an expression vector for *E.coli* equipped with a phage T5 promoter and a double *lac* operator repression module. Via IPTG, high-level expression of a 6xHis fusion-protein, in this case of the C-terminus of HCN2, is induced. For selection in *E.coli*, an ampicillin-resistance gene is included.

Lentivirus Plasmids

The original lentivirus plasmids were provided by the lab of Inder Verma (The Salk Institute for Biological Studies, Laboratory of Genetics, La Jolla, CA, USA).

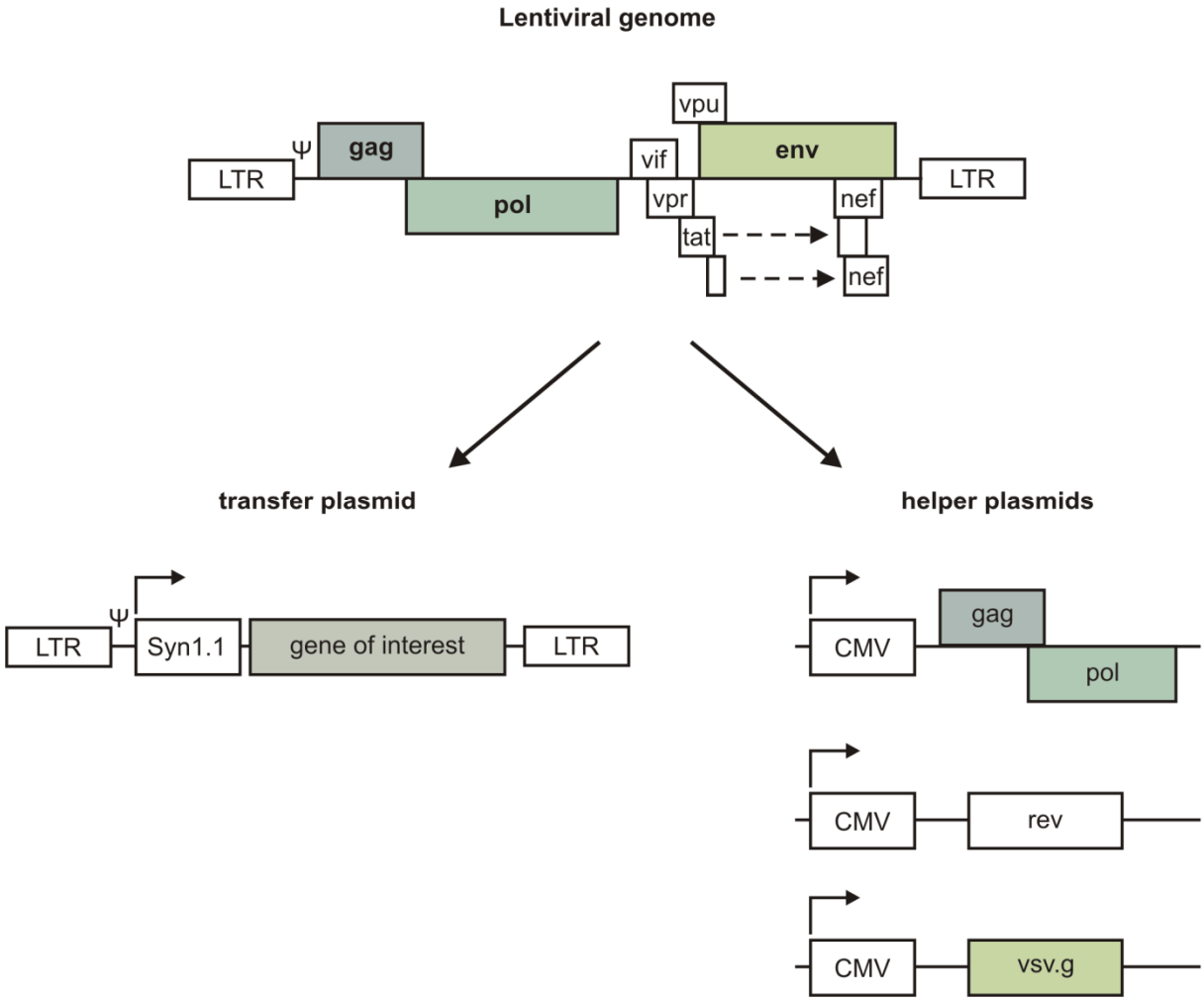

Fig. 5: Cartoon of the HIV-1 genome (upper panel) and the derived lentiviral vector system of the third generation (lower panel). The viral genome was separated into a transfer plasmid (left) and helper plasmids (right). CMV: cytomegalovirus promoter. *env*: gen for coating proteins. *gag*: gen for specific antigens. LTR: long terminal repeats. *nef*: accessory gen. *pol*: gen for integrase and reverse transcriptase. *rev*: regulatory gen. Syn1.1: synapsin1.1 promoter. *tat*: regulatory gen. *vif*, *vpr*, *vpu*: accessory genes. vsv.g: vesicular stomatitis virus g-protein. Lentiviral genome adapted from (Verma and Weitzman 2005)

In order to produce lentiviral plasmids, the third generation of the HIV-1 derived deliver system was used. As a basis of this viral vector system, it is necessary to separate essential viral genes responsible for replication and production of infectious particles from genes responsible for the

pathogenesis of HIV-1. Hence, the native HIV envelope (*env*) is the limiting factor for the use of lentivirus in biological research and therefore it was replaced by coating proteins of heterologous viruses. Commonly, the vesicular stomatitis virus g-protein (*VSV.G*) is used for pseudotyping (Fig. 5) (Verma and Weitzman 2005) which is now located in the helper plasmid pMD.2G. In order to reduce the risk of homologous recombination and the resulting production of infectious particles, the HIV genes *vif*, *vpr*, *vpu* and *nef* were removed from the lentiviral genome (Fig. 5) (Delenda 2004). The *tat* trans-gene is also non-essential for the efficient production of lentiviral vectors and was replaced by a strong heterologous promoter sequence. An essential part is the *rev* gene which interacts with the *rev* response element (RRE) and enhances the export of the unspliced, full-length genome transcripts of *gag-pol* mRNA and the genomic RNA of the transfer vector (Fig. 5) (Delenda 2004). In the vector system, the *rev* gene is located on the pRev and the *gag-pol* on the pMDL, respectively. The latter encodes a gag-pol precursor protein which is processed to an integrase, a reverse transcriptase and structural proteins essential for the lentivirus particle production. The gene of interest is cloned into the transfer vector containing a synapsin specific promoter (Syn1.1) which allows neuron specific expression (Fig. 5 lower left panel) (Dittgen et al. 2004).

2.3 Mouse Lines

In this study, HCN2 and cGKII specific knockout mice were used. The HCN2-deficient mouse line was generated by disrupting the HCN2 gene through homologous recombination using a Cre/loxP-based strategy (Ludwig et al. 2003). As a consequence, the exons 2 and 3 encoding the transmembrane segments 2 to 6 and the pore are deleted. The mating of the HCN2 mouse line was sustained heterozygously.

The same Cre/loxP-based strategy was used for the creation of the cGKII-deficient mouse line (Pfeifer et al. 1996). The disrupted exon 2 encoded the first part of the cGMP binding domain. Animals derived from this mouse line were mated homozygously. All animals have a mixed background of 129SvJ and C57-Bl6/N strains, received food (Ssniff; regular feed: R/M-H, breeding feed: M-Z Extrudat) and water ad libitum and lived in a light-dark cycle of 12 h.

2.4 Working with DNA

2.4.1 Isolation of Genomic DNA for Genotyping

Young mouse tail tip tissue probes (< 21d) were digested with proteinase K (20 mg/ml, Roche) at 55°C over night. The next day, the proteinase K was heat inactivated at 95°C for 10 min and the tissue lysates were used as template in the genotyping polymerase chain reaction (PCR).

10x proteinase K buffer	
100 mM	Tris-HCl, pH 8.0
200 mM	NaCl
5 mM	EDTA
0.2%	SDS

2.4.2 Polymerase Chain Reaction

The method was used for the amplification of genes, correction or deletion of mutations, and genotyping. The conditions of each PCR reaction were adjusted to the respective application. Table 1 shows an overview about the standard PCR conditions of different polymerases. The pipetting scheme of the PCR adapted from the manual of the respective manufacturer.

Table 1: Standard PCR conditions for different polymerases.

Polymerase	**Taq (self made)**	**Pfu (Stratagene)**	**Herculase (Stratagene)**	**Phusion (Finnzymes)**	
Initial denaturation	95°C 1 min	95°C 1 min	95°C 1 min	98°C 30 s	
Denaturation	95°C 30 s	95°C 45 s	95°C 20 s	98°C 10 s	
Annealing	x°C 30 s	x°C 45 s	x°C 20 s	x°C 30 s	35 cycles
Elongation	72°C 30 s/kb	72°C 60 s/kb	72°C 30 s/kb	72°C 30 s/kb	
Final elongation	72°C 5 min	72°C 5 min	72°C 5 min	72°C 5 min	
Storage	10°C ∞	10°C ∞	10°C ∞	10°C ∞	

For genotyping, a multiplex-PCR was used which enables simultaneous amplification of targets of interest in one reaction by using more than one pair of primers. The multiplex-PCR was combined

with a touchdown PCR which is another modification of conventional PCR that may result in a reduction of nonspecific amplification, especially of genomic DNA. It involves the use of an annealing temperature that is higher than the target optimum in early PCR cycles. The annealing temperature is decreased by 1°C every cycle until a specified or 'touchdown' annealing temperature is reached. The touchdown temperature is then used for the remaining number of cycles. This allows for the enrichment of the correct product over any non-specific product.

Genotyping	**HCN2**		**cGKII**		
Initial denaturation	95°C	5 min	94°C	5 min	
Touchdown:					
Denaturation	95°C	30 s	94°C	30 s	
Annealing	71°C, dT -1°C	30 s	66°C, dT -1°C	30 s	10 cycles
Elongation	72°C	30 s	72°C	60 s	
Denaturation	95°C	30 s	94°C	30 s	
Annealing	61°C	30 s	59°C	30 s	25 cycles
Elongation	72°C	30 s	72°C	60 s	
Final elongation	72°C	5 min	72°C	10 min	
Storage	10°C	∞	10°C	∞	

2.4.3 Restriction Analysis and Preparation of Samples for Cloning

All restriction enzymes were acquired from New England BioLabs (NEB) or from Fermentas. Restriction analysis conditions were performed following the manufacturer's instructions.

For cloning, 3-5 µg of DNA were digested usually at 37°C. After the incubation time, the cut DNA was separated electrophoretically and the bands were cut precisely using a scalpel.

2.4.4 Purification of DNA Fragments

After PCR amplification and restriction digest, the PCR fragments were purified for further applications. The purification was performed using the PureLink™ Quick Gel Extraction Kit (Invitrogen) according to manufacturer's protocol. All solutions needed for this procedure were provided with the kit. Briefly, threefold amount of solubilization buffer was added to the excised gel slice. The sample was incubated at 55°C until the gel was completely solved and loaded onto a silica spin column which was placed into a 2 ml Eppendorf tube. The gel extract was centrifuged (13,000 rpm, 1 min) and the flow through was discarded. 700 µl wash buffer was added to the

column followed by an additional centrifugation step. After discarding the flow through, the column was spun in order to remove all ethanol present. Finally, the DNA was eluted with 30 µl ddH_2O or elution buffer into a fresh 1.5 ml Eppendorf tube by centrifugation. The successful purification was verified by agarose gel electrophoresis.

2.4.5 Dephosphorylation and Ligation

The dephosphorylation of the vector and subsequent ligation with the insert were performed with the *Rapid DNA Dephos Ligation Kit* from Roche. A dephosphorylation of the vector was accomplished if only one restriction endonuclease was used. 1 µg of the purified vector DNA was mixed with 10x rAPid alkaline phosphatase buffer and 1 U of rAPid alkaline phosphatase in a total volume of 20 µl. The solution was centrifuged briefly and incubated for 30 min at 37°C. In order to inactivate the rAPid alkaline phosphatase, the reaction was heated up to 75°C for 2 min. For ligation, 50 ng of the dephosphorylated vector was added to 150 ng of the insert, 5x DNA dilution buffer in a volume of 10 µl and mixed thoroughly. 10 µl of 2x DNA ligation buffer and 5 U T4 DNA ligase were supplied to the ligation reaction and incubated for 30 min at room temperature.

2.4.6 Transformation

For transformation, the chemically competent *E.coli* strain XL1 blue (NEB) was used. First, a 100 µl aliquot of competent XL1 blue cells were thawed on ice. Then, 10 µl of the ligation reaction or 20 ng plasmid DNA for retransformation were added to the cell suspension. After an incubation step on ice for 30 min, a heat pulse was performed by incubating the cells for 45 sec at 42°C in a water bath. Immediately after this, the cell suspension was replaced on ice for 2 min. A volume of 900 µl prewarmed Luria Bertani medium containing glucose (LB (+)) was added to the cells and agitated for 1 h at 37°C. The cells were pelleted at 3,500 rpm for 5 min at room temperature and resuspended in 150 µl of LB (+) medium. Finally, the cells were plated on the agar plates containing appropriate antibiotics and incubated over night at 37°C.

antibiotics	
100 µg/ml	ampicillin
30 µg/ml	kanamycin
30 µg/ml	chloramphenicol

LB(+) medium	
10 g	peptone
5 g	yeast extract
5 g	NaCl
1 g	glucose
	adjust pH to 7.2 - 7.5
ad 1 L	ddH_2O, autoclave

LB(+) Agar	
10 g	peptone
5 g	yeast extract
5 g	NaCl
1 g	glucose
15 g	agar
	antibiotics
	adjust pH to 7.2 - 7.5
ad 1 L	ddH_2O, autoclave

2.4.7 Inoculation of Bacterial Cells and Isolation of Plasmid DNA (Alkaline Lysis)

Bacterial clones were picked from the agar plate and transferred to 10 ml polypropylene tubes (VWR) containing the LB (+) medium with the appropriate resistance. Then, the suspension was incubated over night at 37°C with shaking (225 rpm). On the next day, the cells were spun at 1,000 g for 10 min at 4°C and the pellet was solved in 250 µl resuspension buffer. This solution was transferred into 2 ml Eppendorf tubes. After adding 250 µl lysis buffer, the cell suspension was inverted several times and was allowed to incubate for maximal 5 min at room temperature. Then, 250 µl of the neutralization solution was added to the mix, the latter was inverted and incubated 5 min at room temperature. The suspension was centrifuged at maximal rpm for 15 min at 4°C or at room temperature and the supernatant containing the plasmid DNA was transferred into fresh 1.5 ml Eppendorf tubes. To precipitate DNA, 520 µl 100% isopropanol was added to the mix. After vortexing, the mix was spun at rpm maximal for 15 min at 4°C. Subsequently, the pellet was washed with 70% ethanol and the solution was centrifuged at rpm maximal for 5 min at 4°C. Then, the supernatant was discarded and the pellet was dried in a vacuum centrifuge at RT for 5 min. The pellet was suspended in 30 µl of ddH_2O and 1 µl of this plasmid DNA solution was used for the restriction analysis. If expected results were obtained, the corresponding plasmid DNA was send for sequencing without further purification. To yield plasmid DNA in larger amounts and in higher purity, PureYieldTM Plasmid Midiprep System (Promega) was used. For that purpose, colonies were inoculated in 100 ml LB (+) medium and similar procedure as described above was performed following the manufacturer's instructions.

2.4.8 TOPO Cloning

TOPO cloning (TOPO TA Cloning® Kit Dual Promoter, Invitrogen) represents a rapid and convenient cloning method for PCR products. Topoisomerase I from *Vaccinia* virus attached to the pCRII®-TOPO® vector allows for covalent binding of PCR products to this vector. However, this reaction only takes place if the respective PCR product possesses a deoxyadenosine (A) on its 3' end. In contrast to most polymerases with proof reading activity (i.e. Pfu-polymerase), conventional Taq polymerase has terminal transferase activity and adds a single adenosine to the 3´ ends of the PCR products.

First, PCR products which were amplified using a polymerase without terminal transferase activity were purified by standard procedures as described in chapters 2.4.4 and 2.4.3. Then, 8 µl of the purified PCR product was added to 0.5 µl dNTPs (MP biomedicals, 10 mM each), 1 µl Taq buffer (MP biomedicals, containing 2.5 mM $MgCl_2$) and 0.5 µl Taq-polymerase (self-made). This reaction was incubated for 30 min at 72°C and placed on ice afterwards. The TOPO cloning reaction was performed using 4.5 µl of the Taq-polymerase reaction product, 1 µl salt solution and 0.5 µl TOPO vector (both provided with the kit). The mix was incubated for 20 min at room temperature and subsequently 5 µl were transformed into chemically competent bacterial cells (see 2.4.6).

2.4.9 Introduction of Mutations in DNA Constructs

In most cases, mutations were introduced by means of site-directed mutagenesis. Site-directed mutagenesis PCR was performed using the QuikChange XL Site-Directed Mutagenesis Kit (Stratagene) according to manufacturer's instructions. Another method to introduce mutations is the overlap-PCR which needs four primers to introduce mutagenesis. The first pair of primers was used to amplify DNA that contains the WT-template together with upstream sequences (overlap) of the mutation to be inserted. The second pair of primers confines DNA which contains the mutation site and downstream sequence. The two overlapping fragments were mixed, denaturated and annealed to generate heteroduplexes which can then be elongated. In a third PCR the heteroduplexes were amplified into full-length DNA using primers that bind to the extremes of the initial fragments. Over unique restriction sites, a mutated PCR-construct is inserted into the WT-plasmid DNA.

2.4.10 Reverse Transcription (RT)

Reverse transcription was performed using the ThermoScriptTM RT-PCR System Kit (Invitrogen) following the instructions of the manufacturer. During the cDNA synthesis, random hexamers as well as oligo (dT) primer were added to the reaction. After the cDNA synthesis, RNA was degraded using RNAse H and a PCR was performed. The reverse transcription was used to amplify the interacting candidates of HCN2 out of the mouse brain.

2.4.11 Cloning of HCN Channels

Cloning of the mouse HCN2 and human HCN4 subunits was described previously (Ludwig et al. 2003, Much et al. 2003, Zong et al. 2005). A complete primer list is provided in the appendix. If not specified, all experiments from the electrophysiological and biochemical recordings in chapter 2.8 were obtained using mHCN2 subunits. The interacting candidates were amplified from brain or heart cDNA using RT-PCR, cloned into the pcDNA3.1 and/or pIRES-eGFP vector and sequenced.

2.5 Library Screen

The Yeast Two Hybrid Screen (CytoTrap XR® Premade Library Kit, Stratagene) was used to identify putative interacting candidates of the C-terminus of HCN2 in brain tissue using a mouse cDNA library.

2.5.1 Preparation of Yeast cdc25H Competent Cells

To prepare fresh yeast competent cells, some ice splinters were scraped off the cdc25H glycerol stock with a pipetting tip and were plated on a fresh YPAD agar plate. Yeast cells were allowed to grow at room temperature for approx. 4 days (d) or until first visible colonies started to appear. 4-5 of these colonies were picked and were transferred in 50 ml YPAD broth. After mixing this solution thoroughly, it was transferred to a 250 ml flask and incubated at 25°C with shaking until the optical density (OD_{600}) was >1 (this usually took 16-18 h). Then, the yeast solution was diluted in YPAD broth to an optical density of 0.2 and was incubated again at 25°C until OD_{600} was between 0.9-1.1. 75 µl of such cell suspension was plated on an YPAD agar plate which was incubated for 4-7 days at 37°C. This plate served as a control for spontaneously occurring temperature revertants. If more than 30 colonies were present, the results obtained from the competent cells are unusable. The cell suspension (OD 0.9-1.1) was spun down at 1000 g for 5 min at room temperature and washed with sterile water. Then, the pellet was resuspended in 50 ml LiSORB and incubated 30 min at room temperature. Meanwhile, 800 µl salmon sperm DNA (10 mg/ml) were boiled in water bath for 10 min, 200 µl LiSORB were added and the solution was allowed to cool down to room temperature.
After the 30 min incubation, the yeast cell suspension was spun at 1000 g for 5 min at room temperature. The pellet was resuspended in 300 µl LiSORB and 600 µl of the salmon sperm DNA was added followed by 5.4 ml PEG/LiOAc and 530 µl DMSO (Sigma). Prior to the transformation the solution was thoroughly but gently mixed by pipetting.

YPAD broth	
10 g	yeast extract
20 g	bacto peptone
20 g	glucose
40 mg	adenine sulphate
	autoclave

YPAD plates	
10 g	yeast extract
20 g	bacto peptone
20 g	glucose
40 mg	adenine sulfate
20 g	bacto agar
	autoclave

LiSORB	
100 mM	LiOAc
10 mM	Tris-HCl (pH 8.0)
1 mM	EDTA
1 M	sorbitol
ad 1 L	ddH_2O, adjust pH to 8.0
	autoclave

PEG/LiOAc	
100 mM	LiOAc
10 mM	Tris-HCl (pH 8.0)
1 mM	EDTA
40% (w/v)	PEG 3350
	adjust pH to 8.0
	sterile filtrate

2.5.2 Co-transformation of Competent Cells

For library screen, two preparations of competent cells were done in parallel resulting in a final volume of approx. 14 ml. In a 50 ml Falcon tube (Sarsteadt), 40 µg of the pSOS-C-Terminus of HCN2, 200 µl of 1.4 M β-mercaptoethanol and 40 µg of pMyr mouse brain cDNA plasmid library were added to 10 ml of freshly made yeast competent cells. The solution was mixed by inversion and transferred into 20 separate 1.5 ml Eppendorf tubes each containing 500 µl transformation suspension. As a negative control, 2 µg of empty pSOS plasmid, 10 µl of a 1.4 M β-mercaptoethanol solution and 2 µg of pMyr cDNA plasmid library were added to 500 µl of freshly made yeast competent cells. Both were incubated at room temperature for 30 min and mixed occasionally. After the incubation time, the mixtures were exposed to a heat shock at 42°C for 20 min and subsequently placed on ice for 3 min. The cells were collected by centrifugation at 14,000 rpm for 30 sec at room temperature and the pellet was resuspended in 0.5 ml of 1 M sorbitol.

2.5.3 Identification and Verification of Putative Interactors

Transformated cells were plated on 15 cm SD/glucose (-UL) agar plates using approximately 10 non-acid washed glass beads per plate. Then, the glass beads were poured off and the plates were allowed to incubate at 25°C for 3 days. Hereafter, the transformants were replica plated on 15 cm SD/galactose (-UL) agar plates by application of relatively firm pressure. These plates were then incubated at 37°C for several days until first colonies were visible. The SD/glucose (-UL) plates were incubated at 25°C for estimation of the transformation efficiency. The number of clones appearing on the control SD/galactose (-UL) plate incubated at 37°C indicated the temperature sensitive revertants. 6-10 days after the transformation, the clones from the SD/galactose (-UL) plates (at 37°C) were picked and solved in 20 µl sterile ddH_2O. To repress the *GAL1* promoter-driven expression from the pMyr vector, 5 µl of these cells were patched onto a 10 cm SD/glucose (-UL) plate and incubated at 25°C for 2-3 days. After the incubation time, from this plate each of the colonies was patched onto two fresh SD/glucose (-UL) plate and one SD/galactose (-UL) plate. One SD/glucose (-UL) plate was incubated at 25°C, the other SD/glucose (-UL) and the SD/galactose (-UL) plate were incubated at 37°C. After 2-3 days, colonies that appeared on the SD/galactose (-UL) plate (at 37°C) but not on the SD/glucose (-UL) plate (at 37°C) were considered as putative interactors in this primary test. To perform the secondary test, the respective clones from the SD/glucose (-UL) plate incubated at 25°C were re-patched and grown on a fresh SD/galactose (-UL) and SD/glucose (-UL) plate, respectively. These plates were incubated at 37°C and after 2-3 days were inspected for growing colonies. Those colonies growing on the SD/galactose (-UL) plate but not on the SD/glucose (-UL) plate were picked and used for the isolation of plasmid DNA.

SD/Glucose (-UL) Agar Plates	
1.7 g	yeast nitrogen base w/o aa
5 g	ammonium sulphate
20 g	bacto agar
20 g	glucose
ad 900 ml	ddH_2O
	autoclave and cool to 55°C
100 ml	10x dropout solution (sterile)

SD/Galactose (-UL) Agar Plates	
1.7 g	yeast nitrogen base w/o aa
5 g	ammonium sulfate
20 g	bacto agar
20 g	galactose
10 g	raffinose
ad 900 ml	ddH_2O
	autoclave and cool to 55°C
100 ml	10x dropout solution (sterile)

10x Dropout Solution (UL)			
300 mg	L-isoleucine	500 mg	L-phenylalanine
1500 mg	L-valine	2000 mg	L-threonine
200 mg	L-adenine hemisulfate salt	500 mg	L-tryptophan
500 mg	L-arginine HCl	500 mg	L-tyrosine
200 mg	L-histidine HCl monohydrate	1000 mg	L-glutamic acid
500 mg	L-lysine HCl	1000 mg	L-aspartic acid
200 mg	L-methionine	400 mg	L-serine

2.5.4 Isolation of pMyr Plasmid DNA from Interaction Candidates

In order to figure out the molecular identity of the putative interactors, the corresponding pMyr cDNA has to be sequenced. For this purpose, pMyr plasmids were isolated from the respective yeast cells by the following protocol:

First, each of the putative positive colonies from previous step (chapter 2.5.3) was inoculated in a separate 50 ml Falcon tubes containing 5 ml of SD/glucose (-UL) medium and was cultured at 25°C for 2-3 days or until OD_{600} was > 1. Then, the cells were spun at 1000 g for 5 min at room temperature. All solutions used during the next steps were obtained from the QIAprep Spin Miniprep Kit (Qiagen). Now, the pellet was resuspended in 250 µl P1 buffer and transferred into a 1.5 ml Eppendorf tube. Next, 250 µl P2 buffer, 250 µl phenol and a small amount of glass beads (∅ 0.5 mm) were added to this solution. The latter was mixed thoroughly for two times consecutively for 1 min and spun at maximal speed for 10 min at room temperature. The upper aqueous phase was transferred into a separate tube and 350 µl of buffer N3 was added. After inverting this solution, it was spun again at maximal speed for 10 min at room temperature. Subsequently, the supernatant was transferred onto the QIAprep column and centrifuged at room temperature for 1 min at maximal speed. To wash the column, 750 µl Buffer PE was added and the samples were spun again at same conditions. The flow through was discarded followed by an additional centrifugation of the samples to dry the column. Elution of DNA was performed by adding 30 µl EB Buffer to the center of the column and allowing the DNA to solve for 5 min at room temperature. Finally, the samples were spun in new 1.5 ml Eppendorf tubes at room temperature for 1 min at maximal speed. This DNA was used for the transformation in *E.coli* following a standard transformation protocol (see chapter 2.4.6). After plasmid isolation from the obtained bacterial colonies, the respective clones were used for a final interaction test by co-transforming them with the C-terminus of HCN2 in cdc25H yeast cells using a standard transformation protocol. If this interaction test was positive, the respective plasmids were sequenced.

2.6 Cell Culture

2.6.1 Cultivation and Transfection of Mammalian Cell Lines

For most *in vitro* transfections in this study, HEK293 cells or COS7 (both obtained from DMSZ) were used. They were cultivated in DMEM + GlutaMAX™-I medium (GIBCO, + 1 g/l glucose, - pyruvate + 10% FBS + 1% penicillin/streptomycin) at 37°C with 10% CO_2. COS7 cells were cultivated under same conditions in DMEM + GlutaMAX™-I medium (+ 4.5 g/l glucose, + pyruvate + 10% FBS + 1% penicillin/streptomycin).

Transient transfections of HEK293T cells or COS7 cells were performed using the calcium phosphate technique (Graham and van der Eb 1973) or FuGENE® (Roche). For the calcium phosphate based transfection 30 µg DNA was mixed with 260 µl 2.5 M $CaCl_2$ in a total volume of 1300 µl ddH_2O in a 15 ml Falcon tube. 2x BBS solution was added drop wise. Then, the mix was incubated for maximal 5 min at room temperature. This mixture was spirally dropped to the 40-70% confluent cells which were incubated at 37°C with 3% CO_2 subsequently. 8-16 h after the transfection, the medium was replaced and the cells were further incubated at 37°C with 10% CO_2 until harvesting.

Transfection with FuGENE® was performed for subsequent immunocytochemical and electrophysiological applications. For 16-well plates 30 ng DNA per well was used, for 3.5 cm plates 3 µg DNA was used. First, fresh GlutaMAX™-I medium (without FBS and without penicillin/streptomycin) was added to cryotubes followed by the addition of DNA. Thereby, tenfold volume of medium related to the total volume on DNA was added (i.e. 1 µl DNA corresponds to 10 µl medium). After the 5 min incubation, FuGENE was added directly to the reaction which was mixed subsequently by pipetting up and down. In this case, threefold volume of FuGENE in µl was used related to the amount of DNA in µg (i.e. 1 µg DNA corresponds to 3 µl FuGENE). This reaction was incubated 30 min at room temperature and added directly into the medium of the cells. The transfected cells were maintained at 37°C with 10% CO_2 until proceeding with the respective application.

2xBBS	
10.65 g	BES
16.35 g	NaCl
0.21 g	$Na_2HPO_4 \cdot 2H_2O$
	adjust pH to 6.95 with NaOH
ad 1000 ml	ddH_2O
	filtrate sterilely

2.6.2 Primary Hippocampal Neuron Culture

Primary neurons were isolated as described previously (Celis 1994, Fath et al. 2009). A priori, glass coverslips (Ø 18 mm, Marienfeld GmbH) were put in a porcelain staining rack (Thomas Scientific), rinsed with water and left in concentrated nitric acid (65%) over night. The acid was removed by extensive washing with easypure water (6 times, 30 min) and the coverslips were sterilized by dry heat (230°C, 6 h). Afterwards, the sterile coverslips were distributed in culture dishes (35 mm, Greiner Bio-ONE GmbH), covered with 3-4 drops of the poly-L-lysine solution and incubated overnight at room temperature. The day after, the poly-L-lysine solution was aspirated and the coverslips were washed with sterile water for two times.

Borate buffer	
1.24 g	boric acid
1.90 g	sodium tetraborate
ad 400 ml	ddH_2O

Poly-L-lysine solution	
50 mg	poly-L-lysine
ad 50 ml	borate buffer

At the day of dissection, Hank's Buffered Salt Solution (HBSS, Gibco) was prewarmed to 37°C. Prior to use, trypsin-EDTA (Gibco) was thawed to room temperature. Two culture dishes were filled with warm HBSS and disposed under a laminar flow hood. The pregnant BL6N mice on embryonic day 16.5 (E16.5) were killed and the abdomen was sterilized with an excess of 80% ethanol. With sterile forceps, the skin of the abdomen was lifted and with a pair of scissors and a large incision on the midline from the pelvis up to the thorax was made. The abdominal wall was again sterilized with excess of ethanol and the uterus with the embryos was opened. With large forceps, the uterus between two embryos was grasped and the uteral horn was cut from below. The whole uterus was transferred to a dish with HBSS.

In a next step, the embryos were removed from the uterus by cutting the placenta and pulling the embryos out. The embryos were decaptitated and the heads were moved to a new HBSS-filled culture dish. To isolate the brain, the head was placed erectly in the dish and stabilized with the curved forceps just above the nose. With an additional pair of straight forceps the skin was removed (both forceps were obtained from Fine Science Tools GmbH, Dumont SS-45 Forceps - Inox Medical and Dumont #45 Forceps - Dumoxel, respectively). With one tip of the forceps, the skull was punctured along the middle vein and disrupted without damaging the brain. The skull was pulled away and the meninges were removed carefully and completely. The hippocampi were removed under a stereo-microscope (Stemi 2000, Zeiss). The brain was placed dorsally in the culture dish and

stabilized with the straight forceps in the cerebellum. The curved forceps were used to cut away the two hemispheres, and the rest of the brain was discarded (Fig. 6A). The hemisphere was laid on the lateral side with the internal side facing up. The meninges which can be identified by tiny blood vessels had to be removed completely by pulling it gently away. Then, the hippocampus was visible immediately being located in the rostral part of the hemisphere and having a banana-like shape (Fig. 6B). The inner side was free to access. To isolate the hippocampus, two cuts had to be done, the first at the dorsal side towards the hippocampus and the second one at the ventral end of the hippocampus. After that, the hippocampus could easily be turned down and could be isolated by cutting along the convex outer side.

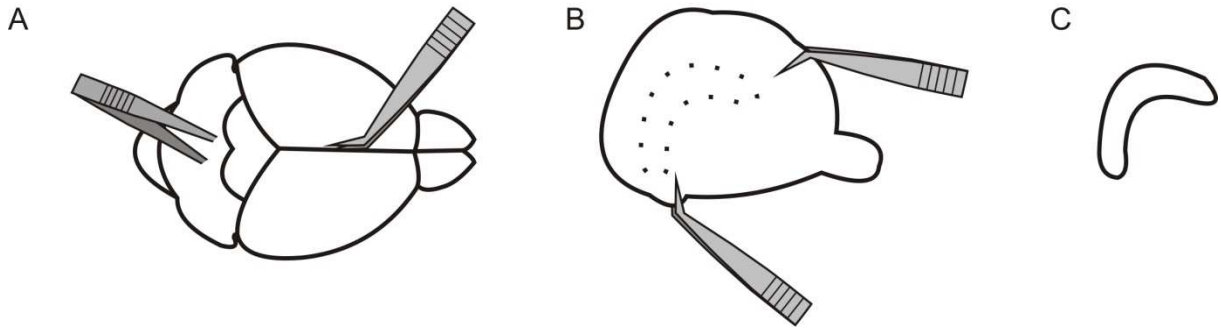

Fig. 6: Dissection of embryonic hippocampus. Adapted to de Hoop, 1994.

All dissected hippocampi were collected in a new culture dish containing warm HBSS, transferred to a conical tube and as much HBSS as possible was removed. The trypsin (Gibco) was added and the hippocampi were digested for 15 min at 37°C. Subsequently, the trypsin solution was subducted, washed for three times in HBSS and dissociated in 1.5 ml HBSS by pipetting up and down with a Pasteur pipette. After the solution became cloudy, the Pasteur pipette was changed to a fire polished one and the tissue was dissected until all clumps broke. On one poly-L-lysine treated plate, approximately 150,000 cells were plated. After settling of 5 min, N-MEM was added to the culture dishes. The primary hippocampal neuron culture was maintained at 36.5°C and 5% CO_2.

HBSS	
500 ml	HBSS (Gibco)
5 ml	Pen/strep (10,000 U/ml)
0.7 ml	1 M HEPES-NaOH, pH 7.35

Trypsin-EDTA	
100 ml	0.05% Trypsin-EDTA (Gibco)
1 ml	Pen/strep (10,000 U/ml)
1 ml	1 M HEPES-NaOH, pH 7.35

N2 supplement	
5 ml	insulin (5 mg/ml)
5 ml	progesterone (20 µM)
5 ml	putrescine-dihydrochloride (100 mM)
5 ml	selenium-dioxide (30 mM)
500 mg	apo human transferring
480 ml	N-MEM
	filtrate sterilely, aliquot à 50 ml

N-MEM	
405 ml	Sigma H_2O
50 ml	10x MEM (Gibco)
20 ml	5.5% $NaHCO_3$
15 ml	20% D(+)glucose anhydrate
5 ml	glutamine (200 mM)
5 ml	pyruvate (11 mg/ml)
	filtrate sterilely

On day two after plating, the primary neuron culture was transfected with the lentivirus containing either cGKII-myc fusion protein or the HCN2 channel. All animal procedures were conducted in accordance to the German animal protection laws and the guidelines of the DFG.

2.6.3 Production of Lentiviral Vectors

The lentivirus particles were prepared by quadruple transfection of HEK293T cells (Tiscornia et al. 2006). The maintenance of HEK293T cells is described in section 2.6.1. Twelve plates with HEK293T cells of 60% confluence were transiently transfected by the calcium phosphate method according to the following scheme.

Transfection Mix	
216 µg	transfer plasmid
140 µg	pMDL
61.6 µg	pREV
58.4 µg	pMD2.G
1.4 ml	$CaCl_2$
ad 14 ml	ddH_2O

The day after transfection, the medium was renewed. The harvest of the lentivirus was performed on the two subsequent days. For the first harvest, the virus containing medium was filtered (CA filter, 45 µm, Sarstedt) to get rid of cell debris. The flow through was centrifuged in an ultra-centrifuge (Coulter-Beckmann, SW 28 rotor) for 2 h at 19,400 rpm and 17°C in swing-out buckets. The pellet was

solubilised in HBSS and stored over night. For the second harvest, the procedure mentioned above was repeated. The HBSS containing virus solutions from the first and second harvest were combined. To concentrate the virus, it was again centrifuged in a 20% sucrose solution (Coulter-Beckmann, SW 55 rotor) for 2 h at 21,000 rpm and 17°C in swing-out buckets. The pellet was resuspended in 100 µl HBSS and stored in 5 µl aliquots at -80°C until use. For transduction of primary neurons, the volume of medium was halved and the amount of virus was determined empirically. The day after transduction, the medium was renewed and adjusted to 3 ml.

2.7 Protein Biochemistry

2.7.1 Isolation and Quantification of Proteins

Proteins were isolated from cultured mammalian cells by following protocol: 48 h after transfection, medium was removed and the cells were harvested in a 1.5 ml Eppendorf tube. Then, the cells were collected by centrifugation (4°C, 5 min, 1,000 g). Hereafter, the pellet was resuspended in lysis buffer and rotated at 4°C for 30 min. Subsequently, the cells were spun at 4°C for 10 min at maximal rpm and the supernatant was transferred into a fresh 1.5 ml Eppendorf tube.

For protein isolation mouse tissue was suspended in lysis buffer containing the proteinase inhibitor cocktail mix (Complete EDTA-free, Roche) and the tissue was disrupted using the Potter S homogenizer with 9,000rpm and 10 strokes (B. Braun Biotech International). Then, the suspension was centrifuged at 4°C at 13,000 rpm and the supernatant was transferred into a fresh 1.5 ml Eppendorf tube. To determine the concentration of isolated proteins, a Bradford assay was performed (Bradford 1976). Thereby, 5 µl of the protein solution (5 µl lysis buffer served as blank control) was transferred into 1 ml plastic cuvettes followed by an addition of 95 µl 0.15 M NaCl solution. Then, 1 ml coomassie blue solution was added and after 2 min the protein concentration was measured using the Bradford assay program on the BioPhotometer (Eppendorf). The corresponding calibration curve was performed using BSA as protein standard.

1x Lysis Buffer	
10 ml	1M Tris-HCl, pH 7.4
2 ml	Triton X-100
6 ml	5 M NaCl
2 ml	100 mM EDTA
ad 200 ml	ddH_2O

Coomassie Blue Solution	
50 mg	coomassie brilliant blue G250
25 ml	95% ethanol
50 ml	85% phosphoric acid (H_3PO_4)
ad 500 ml	ddH_2O

2.7.2 Western Blot

Western blot was performed by standard procedures. The protein was transferred to a PVDF membrane (Millipore, pore size 0.45 µm), equilibrated with methanol and blocked in 5% milk powder for 1 h at room temperature with shaking. Then, the incubation of the membrane with the appropriate primary antibody was performed. The optimal incubation time and antibody concentration was determined empirically. Hereafter, the membrane was washed three times in TBST for 5 min followed by 1-2 h incubation with the secondary antibody at room temperature with rotation. Now, the membrane was washed 3-4 times with TBST for 5 min and once in ddH_2O. After the incubation with the luminol reagent according to manufacturer's protocol (Millipore or Santa Cruz), the membrane was put into a film cassette, exposed to an X-ray film (Fuji) and developed in an X-ray film processor (Curix 60, Agfa). The optimal exposure time was determined empirically.

10x TBS	
12.1 g	Tris-HCl
80.2 g	NaCl
ad 1 L	ddH_2O

1x TBST	
100 ml	10x TBS
1 ml	tween-20
ad 1 L	ddH_2O
	protect from light

1x Lysis Buffer	
10 ml	1M Tris-HCl, pH 7.4
2 ml	Triton X-100
6 ml	5 M NaCl
2 ml	100 mM EDTA
ad 200 ml	ddH_2O

Coomassie Blue Solution	
50 mg	coomassie brilliant blue G250
25 ml	95% ethanol
50 ml	85% phosphoric acid (H_3PO_4)
ad 500 ml	ddH_2O

2.7.3 GST Pulldown Assay

To verify the putative HCN2 interaction found in yeast, GST pulldown assays were performed. For this purpose, the HCN2-CT was cloned into the pQE30 vector and the interacting candidates into the pET41a vector.

To express the GST fusion proteins, 5 ng plasmid-DNA was added to BL21 *E.coli* (Novagen). The mix was heat shocked for 30 s at 42°C and incubated on ice for 2 min. The transformed bacteria was incubated for 1 h at 37°C, appropriate antibiotics was added (ampicillin: HCN2-CT; kanamycin: interacting candidates), and the bacterial solution was grown over night in a volume of 7 ml YT-

medium. The next morning, 2 ml of the overnight culture was transferred to 300 ml YT-medium and incubated with shaking until an OD of 0.6-0.8 was reached. Then, the protein expression was induced by the addition of 3 ml 0.1 M Isopropyl-β-D-thiogalactopyranosid (IPTG) stock solution. The bacterial suspension was further incubated with shaking for additional 4 h.

The bacteria were harvested by centrifugation at 5.000 rpm at 4°C for 10 min. The pellet was resuspended in 12 ml ST buffer and 120 µl lysozyme in a 50 ml tube and the mix was lysed for 15 min on ice. 78 µl dithiothreitol (DTT) stock solution was added and the latter was again incubated on ice for 10 min. Cell lysis was performed by addition of 1700 µl N-lauroylsarcosine stock solution, subsequent vortexing, and incubation on ice for 30 min. The lysed cells were sonificated with 30% power in six 40 s steps interrupted by 10 s pause. The cell debris was removed by centrifugation at 8500 rpm at 4°C. The supernatant contained the extracted fusion proteins which were aliquoted and stored at -80°C.

The GST pulldown assay was performed with 500 µl HCN2-CT combined with 500 µl GST fusion protein of the putative interacting candidate. Glutathione-Sepharose beads (4G, GE healthcare) were washed for three times in GST washing buffer to remove the ethanol for preservation. The beads were resuspended in an equal volume of ST-buffer and 100 µl of the washed beads were added to the combined, purified proteins. The mixture was shaken end-over-end over night at 4°C. To remove all non-bound protein, beads were precipitated (2000 rpm, 4°C, 2 min) and the supernatant was discarded. The Glutathione sepharose beads were washed for three times with GST washing buffer and in the end resuspended in 100 µl ST buffer. A volume of 10 µl was used for a control SDS-PAGE gel which was fixed with coomassie staining solution in a microwave until the solution starts to boil. After destaining, the IPTG-induced protein bands appeared. For western blot analysis, 50 ml of the GST pulldown assay was loaded on a SDS-PAGE gel, transferred to a PVDF membrane and the HCN2-CT was detected using the α-HCN2 L antibody.

YT-medium	
16 g	Peptone
10 g	yeast extract
5 g	NaCl
ad 1000 ml	ddH_2O
	adjust pH to 7.0

ST buffer	
50 mM	Tris-HCl pH 8.0
150 mM	NaCl
ad 500 ml	ddH_2O
	adjust pH to 8.0

Lysozyme (10 mg/ml)	
10 mg	lysozyme
ad 1 ml	ddH_2O

DTT stock solution (1M)	
0.77 g	dithiothreitol
ad 10 ml	ST buffer

GST washing buffer	
20 mM	Tris-HCl pH 8.0
200 mM	NaCl
1 mM	EDTA
0.5%	nonidet-40

N-lauroylsarcosine stock solution (10%)	
2 g	N-lauroylsarcosine
ad 20 ml	ST buffer

Coomassie staining solution	
1 g	coomassie blue R250
45%	methanol
10%	acetic acid 100%
ad 1000 ml	ddH_2O

Coomassie destaining solution	
10%	methanol
10%	acetic acid 100%
ad 1000 ml	ddH_2O

2.7.4 Co-Immunoprecipitation

To analyse protein-protein interactions, co-immunoprecipitation experiments using protein G dynabeads (Invitrogen) were performed.

6x Lämmli	
7 ml	4x Tris-HCl/SDS pH 6.8
3 ml	glycerol
1 g	SDS
1.2 mg	bromphenol blue
ad 10 ml	ddH_2O

6x Lämmli + DTT	
7 ml	4x Tris-HCl/SDS pH 6.8
3 ml	glycerol
1 g	SDS
1.2 mg	bromphenol blue
930 mg	DTT
ad 10 ml	ddH_2O

First, approx. 5 µg antibody and PBS were added to 30 µl dynabeads up to a final volume of 500 µl. This solution was rotated for 30 min at 4°C and, subsequently, the supernatant was removed using a magnet to retain the magnetic beads followed by a wash step with 200 µl PBS. Then, 1 mg of the protein lysate was added to the beads and the reaction was filled up with PBS to a final volume of 500 µl. Now, the suspension was rotated for 30 min at 4°C followed by three washing steps with PBS.

After the last wash, the suspension was transferred into fresh 1.5 ml Eppendorf tubes and the supernatant was removed completely. Beads were resuspended in 6x Lämmli buffer (with or without DTT, depending on the application) and incubated at 70°C for 15 min. Finally, the supernatant was loaded on a SDS PAGE gel.

2.7.5 GFP-Trap

The GFP-Trap system (Chromotek) is a tool for the immunoprecipitation of GFP-fusion protein from cellular extracts. Thereby, a GFP-fragment is coupled to agarose beads. The GFP-trap beads were equilibrated in wash buffer and precipitated by centrifugation at 5,300 rpm for 2 min at 4°C. 1 mg protein was added to the beads and the immunoprecipitation was incubated for 2 h with gentle end-over-end shaking at room temperature. Afterwards, the beads were collected by centrifugation and the remaining supernatant was discarded. The pellet was washed two additional times with ice cold wash buffer and resuspended in 20 ml PBS. The SDS-PAGE analysis and western blotting was determined as described above.

Wash buffer	
10 mM	Tris-HCl, pH 7.5
150 mM	NaCl
0.5 mM	EDTA
	PI freshly added

2.7.6 Kinase Assay

The procedure of the *in vitro* kinase assay was described previously (Ammendola et al. 2001). COS-7 cells were transiently transfected by the calcium phosphate method with HCN2-pcDNA3 and several mutants (HCN2-S641A, HCN2-756STOP) in the presence or absence of cGKII-pcDNA3. To obtain cell lysates, cells were washed twice with PBS and then harvested in using a cell scraper. After centrifugation, cells were suspended in hypoosmotic lysis buffer (10 mM K_3PO_4, pH 7.4). Complete cell destruction was done by three times passing through a 27-gauge syringe needle (Braun) and a freeze–thaw cycle. Lysates containing 30 µg of protein were incubated in 50 mM MES pH 6.9, 10 mM NaCl, 1 mM MgAc, 0.4 mM EGTA, 0.1% Triton X-100 and 3 µM 8-pCPT-cGMP. The reaction was started by adding 0.1 mM [γ-^{32}P]ATP (2,000 cpm/pmol, PerkinElmer). After incubation for 15 s up to 10 min at 30°C, the reaction was stopped by addition of Lämmli buffer and denaturated at 95°C for 5 min. Proteins were separated by SDS-PAGE and blotted to PVDF. Incorporated radioactivity was visualized by autoradiography and phosphoimage analysis (BASReader 2.9, Raytest).

2.7.7 Immunofluorescence

Immunofluorescence was performed for COS7 cells, primary hippocampal neurons and coronal brain slices. For all stainings, the specimen were fixed in 4% paraformaldehyde (PFA) for 5 min, permeabilised with Triton-X100 and blocked for 1 h. The incubation with primary antibodies was accomplished over night, followed by extensive washing and secondary antibody incubation. For brain slices, endogenous peroxidases were inactivated by H_2O_2 and the secondary antibody signal was amplified by tyramide (TSA, Perkin Elmer). For the staining of cells, the secondary antibody was incubated at room temperature for 1 h. The cell nuclei were counterstained with Hoechst end the specimen was embedded in mounting medium (Beckman Coulter). Table 2 provides information about the composition of the individual solutions for the staining of COS7 cells, primary hippocampal neurons, and coronal brain slices. All chemicals were diluted in ice cold PBS.

Table 2: Composition of the individual solutions used for immunological staining

	COS7 cells	primary neurons	brain slices
Postfix	4% PFA	4% PFA, 4% sucrose	4% PFA
Quenching	-	50 mM NH_4Cl	-
Blocking / Permeabilization	10% chemiblocker (CB) / 0.3% Tx-100	2% FBS, 2% BSA, 0,2% fish gelatine	10% NGS / 0.3% Tx-100
1st AB solution	5% CB, 0,2% Tx-100	5% CB	5% NGS, 0,2% Tx-100
2nd AB solution	2% CB	2% CB	2% NGS

2.8 Electrophysiological Recordings

All experiments obtained from electrophysiological recordings in this study were performed by PD Dr. Xiangang Zong as described previously (Biel et al. 1994, Biel et al. 1996, Sautter et al. 1998).

Currents of heterologous expressed HCN channels were measured at room temperature 2-3 days after transfection using the whole cell voltage clamp technique. The extracellular solution was composed of (in mM): 110 NaCl, 0.5 $MgCl_2$, 1.8 $CaCl_2$, 5 HEPES, 30 KCl, pH 7.4 adjusted with NaOH. The intracellular solution contained (in mM): 130 KCl, 10 NaCl, 0.5 $MgCl_2$, 1 EGTA, 5 HEPES, pH 7.4 adjusted with KOH. Pipettes were pulled from borosilicate glass capillaries (GC150TF, Harvard Apparatus LTD) and had resistances of 2-3 MΩ when filled with the intracellular solution. The cGMP-dependent protein kinase inhibitor KT5823 was purchased from Cayman chemicals. A 1 mM stock

solution was prepared in ethyl acetate and was freshly diluted to a final concentration of 1 µM in extracellular solution before use.

2.9 Statistics

Statistical analysis was performed with Origin6.1 (OriginLab) in a one-way ANOVA. Data are presented as mean ± S.E.M. (*n* = number of recorded cells). Values of $p < 0.05$ were considered significant.

3 Results

Analogous to other ion channels, HCNs form multimolecular complexes which consist of a central pore loop and accessory proteins that control the channel properties. These accessory proteins may directly regulate channel activity or influence the targeting properties of HCN channels within a cell. The aim of this study is to identify and characterize interacting proteins of HCN channels in neurons.

3.1 Identification of Interacting Candidates with the HCN2 C-terminus via CytoTrap

As a basis, the HCN2 subunit was chosen as the bait protein since it represents the predominant HCN channel isoform in the brain. In order to identify new regulatory proteins of the HCN2 channel subunit, a CytoTrap (Stratagene) yeast two hybrid screen was performed. The screen was performed using an expression cDNA library from the mouse brain (CytoTrap XR Mouse Brain cDNA Library, Stratagene).

Competent cells of the temperature sensitive cdc25H yeast strain were co-transformed with the C-terminus of the HCN2 channel fused to hSOS and a mouse brain cDNA-library, and were grown at room temperature until the first colonies appeared. After replica plating and selective growth at 37°C, all colonies survived that could rescue their RAS cascade by interaction of the hSos of the bait with a protein of the brain library. Every colony was subsequently spotted on three different plates: two SD/galactose (-UL) plates and one SD/glucose (-UL) plate. A putative interacting candidate was determined as growth on SD/galactose (-UL) plates but not on SD/glucose (-UL) plates at 37°C (Fig. 7, left and middle panel). The growth on galactose plates at room temperature served as positive control (Fig. 7, right panel). In two independent yeast two hybrid screens, about 400,000 yeast cells were screened, 1394 clones were picked and ten putative HCN2-interacting proteins (Hip) could be identified (Fig. 7).

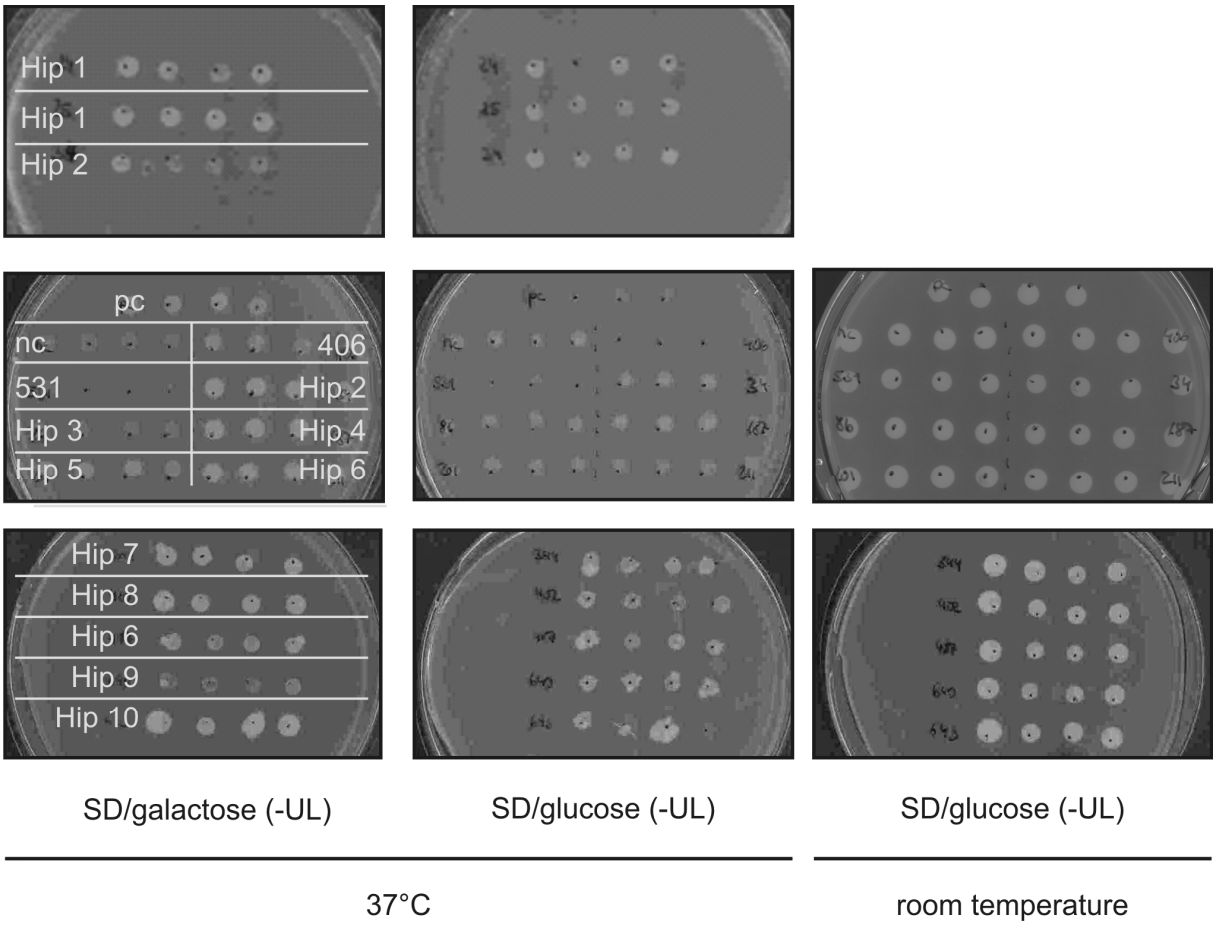

Fig. 7: Putative HCN-interacting proteins in an Y2H screen. Competent yeast cells were co-transformed with a fusion protein consisting of hSOS and the C-terminus of HCN2 and with the mouse brain library. The growth of yeast cells on uracile and leucine-deficient galactose agar plates (SD/galactose (-UL)) at 37°C indicated the rescue of the RAS cascade and, hence, an existing interaction of the HCN2-CT with one of the proteins represented in the library (left and middle panel). SD/glucose (-UL) plates grown at 37°C served as negative control (middle panel), those grown at room temperature served as positive control, respectively (right panel).

3.2 Self Induction

To exclude the possibility that the RAS signalling cascade was induced by the putative interacting candidate alone, the empty pSOS vector was co-transfected with the isolated pMyr vector encoding for the interacting candidate. Self induction was detected if the interacting protein was able to grow without a bait on SD/galactose (-UL) but not on SD/glucose (-UL) plates. Thereby, the HCN2-interacting proteins 1, 2, 4 and 8 showed growth at 37°C on SD/galactose (-UL) plates and no growth on SD/glucose (-UL) plates (Fig. 8). The clones which exhibited self induction were disallowed and not further characterized. All other interacting candidates were specified in the sequel.

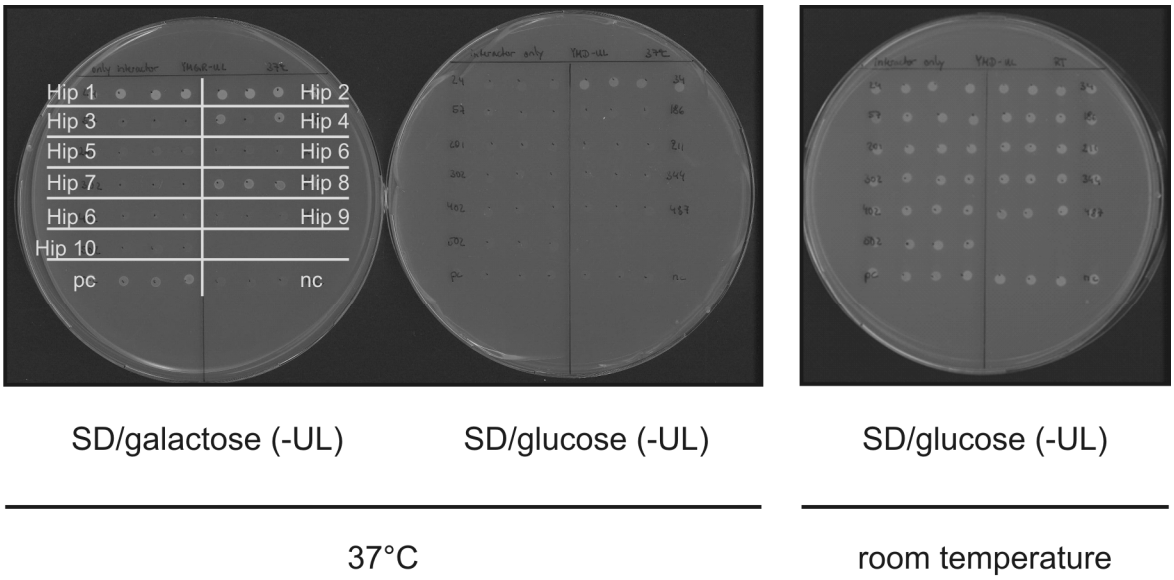

Fig. 8: Self induction of putative HCN-interacting proteins. The putative interacting candidates of the HCN2 C-terminus were transformed with the empty pSOS vector into competent yeast cells. Self induction was determined as growth on SD/galactose (-UL) plates but not on SD/glucose (-UL) plates at 37°C (left panel). All yeast cells were viable as demonstrated by the growth on SD/glucose (-UL) plates at room temperature (right panel).

3.3 Verification of Interacting Candidates with the HCN2 C-terminus via GST-Pulldown

The interacting candidates were tested in a bacterial overexpression system using a Glutathion S-transferase (GST) pulldown assay in order to confirm the interaction between the putative interactors and the HCN2 C-terminus (HCN2-CT). The HCN-interacting proteins were expressed as GST fusion proteins and protein pulldown was performed using GST beads. The IPTG induction was examined in a SDS-PAGE gel stained with coomassie blue (Fig. 9, left panel). The same probes were blotted and stained with an α-HCN2L antibody.

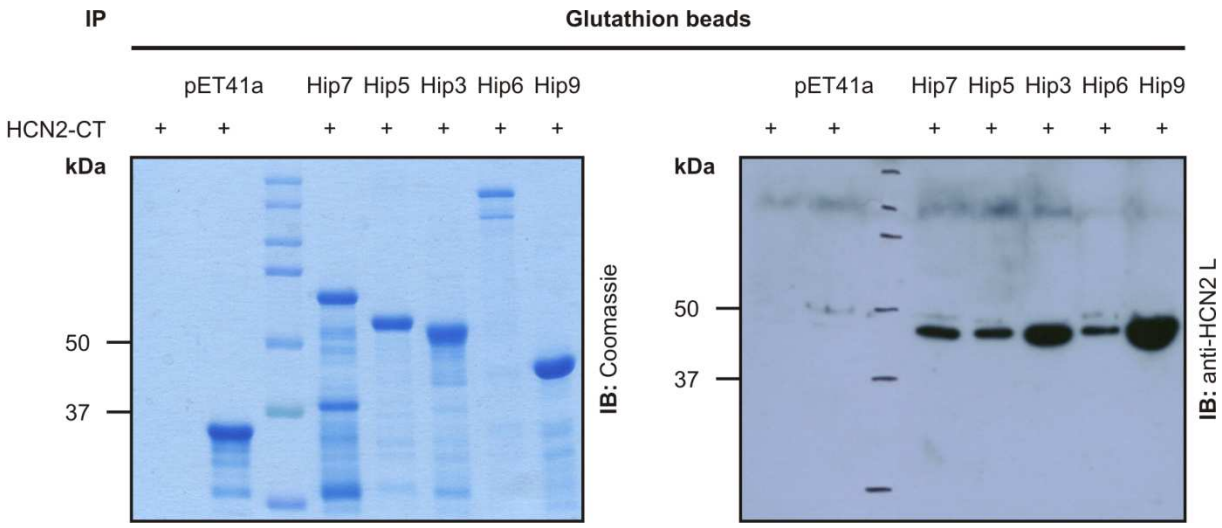

Fig. 9: GST pulldown of HCN-interacting proteins. Proteins were expressed in BL21 *E.coli* after IPTG induction which was examined by coomassie blue staining (left panel). After protein purification, the protein of the HCN2 C-terminus was combined with one of the GST-tagged interacting candidates. The GST-tagged proteins were precipitated using Glutathion Sepharose beads. The interaction with the HCN2 C-terminus was verified in western blot analysis using an α-HCN2L antibody (right panel). 600 µg protein was applied per lane. The HCN-CT and the GST-tagged gene product of the empty pET41a vector together with the HCN-CT, respectively served as negative control.

In the GST pulldown assay, a dominant band at 48 kDa was visible corresponding to the HCN2-CT indicating an interaction of the Hips 3, 5, 6, 7 and 9 with the HCN2-CT (Fig. 9, right panel). It is noteworthy that the HCN2 C-terminus alone did not bind to the Glutathion beads (Fig. 9, right panel, first lane). Additionally, the HCN2-CT did not interact with the GST-tag expressed in the empty pET41a vector (Fig. 9, right panel, second lane). These last two experiments served as negative controls.

3.4 Verification of Interacting Candidates with the HCN2 via CoIP Experiments

To further confirm the interaction, a mammalian expression system was used. HEK293 cell protein lysates expressing myc-tagged HCN-interacting proteins in presence or absence of the HCN2 channel were immunoprecipitated with an anti-myc antibody. Subsequent western blot analysis showed a specific HCN2 signal at about 100 kDa. The HCN2 band was not present in lysates expressing the HCN-interacting protein alone. These results indicate that the full-length HCN channel does also interact with the HCN-interacting proteins 3, 5, 6, 7 and 9 in a mammalian expression system.

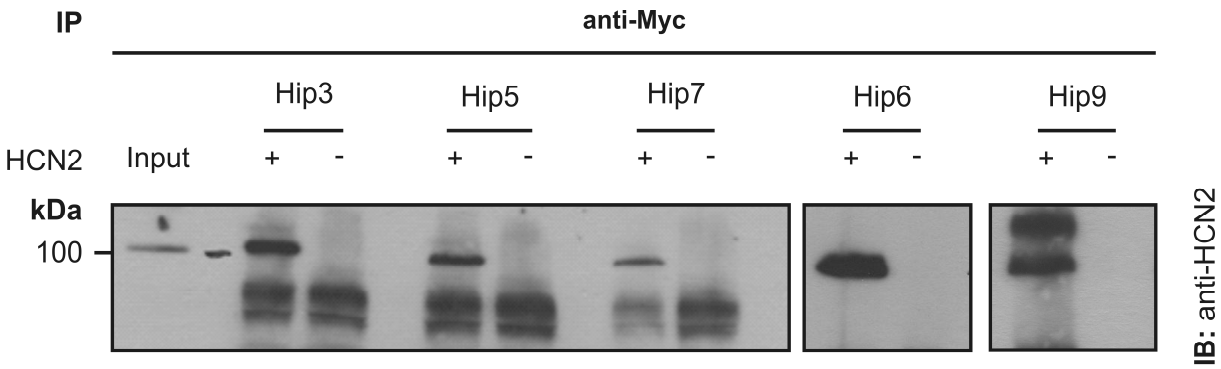

Fig. 10: Interaction between HCN2 and Hip. Co-immunoprecipitation of full length HCN2 and one Hip in HEK293 cells. Lysates of HEK293 cells transfected with HCN2 and Hip 3, 5, 6, 7 or 9 or Hip alone were immunoprecipitated (IP) using a myc antibody and stained for HCN2. 500 µg protein was applied per lane. IP: immunoprecipitation, IB: immunoblot.

3.5 Immunocytochemistry of the HCN-Interacting Proteins and HCN2

In order to receive a better understanding of the molecular basis behind the interaction of the single Hips with the HCN2 subunit, the subcellular localization of the Hips was determined. COS7 cells were transfected with the HCN2 channel and one of the interacting proteins using FuGene. Subsequently, ICC was performed with cyanine dye-conjugated secondary antibodies which showed expression of the HCN-interacting proteins in different subcellular organelles and distinct co-localization (Fig. 11). Whereas the interacting protein 9 shows an almost complete co-localization with the HCN2 channel, the Hip 3 and Hip 5 are only co-localized to some extent. With respect to their subcellular localization, the Hips differ from each other. Hip 6 and Hip 7 show a staining similar of this of scaffold proteins (Fig. 11C- E). The Hips 3, 5 and 9 could not be associated to a certain subcellular compartment (Fig. 11A, B and F). The HCN-interacting protein 9 seems also feasible to upregulate the protein expression of the HCN2 channel (Fig. 11F). To confirm the localization, it is crucial to include protein markers specific for distinct organelles within the cell.

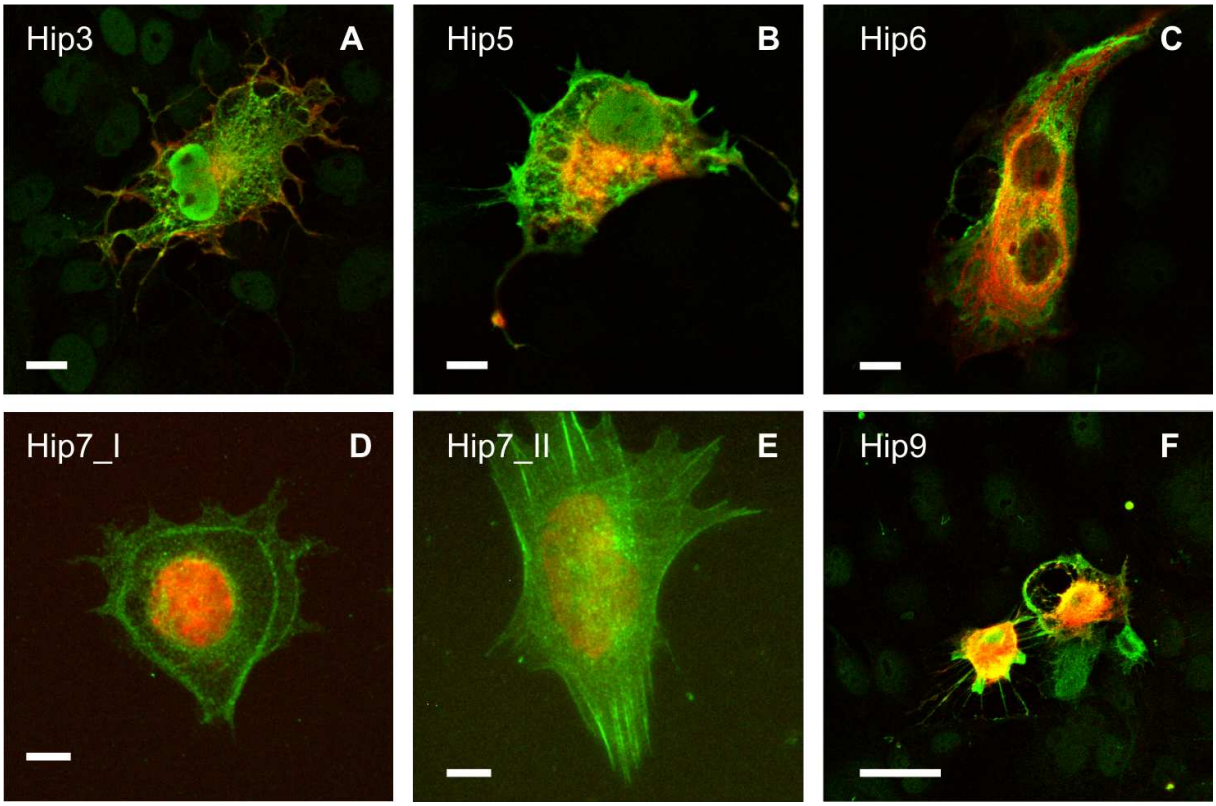

Fig. 11: Co-localization of HCN-interacting proteins in COS7 cells. (A-F) Co-localization in COS7 cells which were transfected with HCN2 and different HIP-myc constructs, respectively. COS7 cells were stained with antibodies against myc (green) and HCN2 (red). Pictures are presented as merge. Scale bar corresponds to 10 µm.

Taken together, the CytoTrap Y2H screen generated several promising interacting candidates of the HCN2-CT which could influence the HCN channel transport, the protein expression or the functional properties of the channel during gating.

3.6 The HCN2 Channel Interacts with cGKII via the CNBD

The activation of HCN channels by cyclic nucleotides was described previously (1.3). In this part of the study, the role of cGMP-dependent regulation was focused. The cGMP-dependent protein kinase was known to be activated by cyclic nucleotides as well. To identify an interaction with HCN channels, the HCN2 subunit and the cGKII were co-expressed in HEK293 cells. Upon co-immunoprecipitation (Co-IP) with an anti-cGKII antibody, a 100 kDa band corresponding to HCN2 was detected in immunoblots (Fig. 12A). To verify a specific interaction of the two proteins Co-IP experiments were performed with anti-cGKII antibody in lysates from mouse hypothalamus, a brain region known to express both HCN2 and cGKII (Ludwig et al. 1998, Werner et al. 2004). Again, a specific HCN2 band was detected (Fig. 12B, left lane) confirming an *in vivo* interaction of HCN2 and cGKII. Importantly, the HCN2 band was not present in hypothalamic tissue from HCN2-deficient mice (Fig. 12B, right lane).

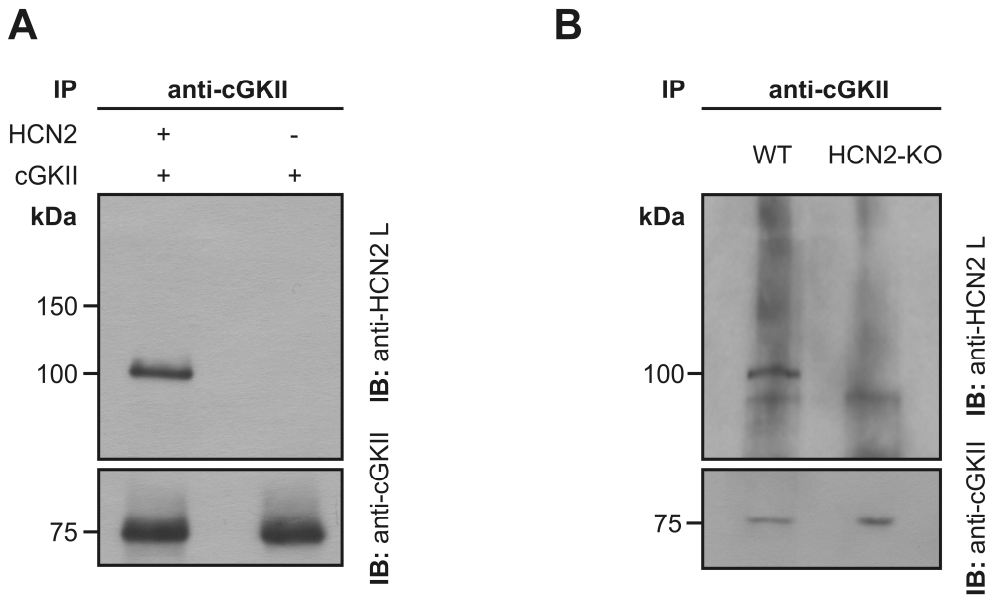

Fig. 12: Interaction between HCN2 and cGKII. (A) Co-immunoprecipitation of HCN2 and cGKII in HEK293 cells. Lysates of HEK293 cells transfected with HCN2 and cGKII or cGKII alone were immunoprecipitated (IP) using a cGKII antibody and stained for HCN2 and cGKII as loading control. 500 µg protein was applied per lane. **(B)** Protein extracts of hypothalamic brain tissue from WT and HCN2-KO mice were immunoprecipitated using a cGKII antibody and analyzed in immunoblots (IB) for HCN2. Anti-cGKII served as loading control.

To further narrow down the region of HCN2 that interacts with cGKII, Co-IPs with GFP-tagged cGKII and myc-proteins corresponding to the combined C-linker/cyclic-nucleotide binding domain (L+CNBD, aa 443-647), the C-linker (L, aa 443-525) or the distal C-terminus of HCN2 channel (dC, aa 647-863) were performed (Fig. 13A, B). Specific bands were obtained for the combined C-linker/CNBD region (Fig. 13B, left lane) while no interaction was found for the C-linker alone

(Fig. 13B, middle lane) as well as for the sequence downstream of the cyclic-nucleotide binding domain (Fig. 13B, right lane). Together, these findings indicated that the CNBD is required for the interaction with cGKII, either alone or in conjunction with the C-linker.

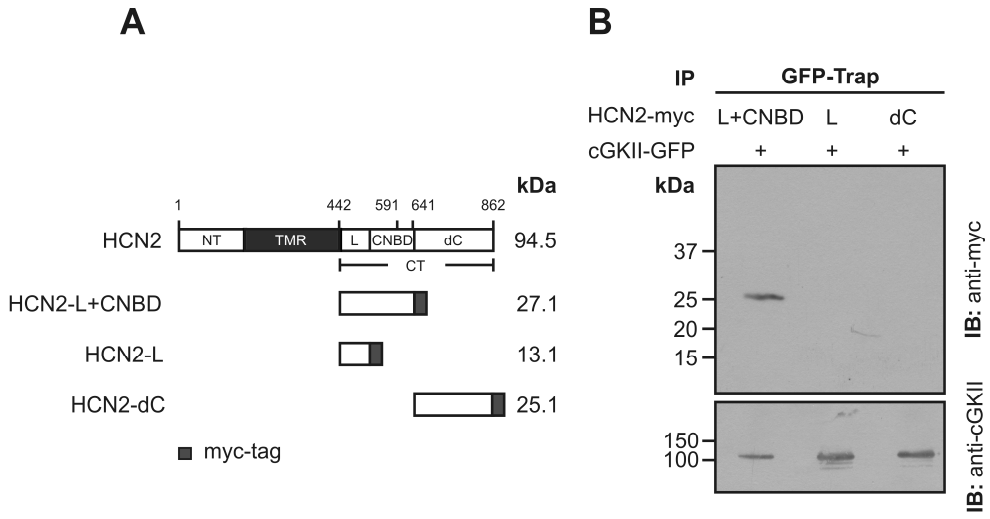

Fig. 13: GFP-Trap. (A) Schematic representation of full length HCN2 (862 amino acids) and myc-tagged HCN2-domains used for interaction studies. The calculated molecular size of the proteins is indicated. TMR, transmembrane region; CT, complete HCN2 C-terminus; L, C-linker; CNBD, cyclic nucleotide-binding domain; dC, distal C-terminus. **(B)** Lysates of HEK293 cells co-expressing cGKII-GFP and myc-tagged portions of the HCN2 C-terminus were bound to GFP-tagged beads. Co-immunoprecipitated proteins were detected by immunoblotting with an anti-myc antibody. Anti-cGKII was used as loading control.

3.7 HCN2 and cGKII Co-localize in Primary Neurons and the Hypothalamic Region

In order to study the subcellular localization of cGKII and HCN2, primary hippocampal neurons were co-transduced with recombinant lentiviral particles expressing the HCN2 and a cGKII-myc fusion protein, respectively. Subsequent immunocytochemical staining showed co-localization of the two proteins at the plasma membrane (Fig. 14A-C). In the absence of primary antibodies immunostaining was not observed, demonstrating the specificity of the antibodies used (Fig. 14D). High levels of cGKII mRNA have been reported to exist in the hypothalamic region, especially in the preoptic nucleus (Werner et al. 2004). In agreement with this, the cGKII protein was identified in coronal slices of the hypothalamic region of wild type mice (Fig. 14E). Stainings performed in consecutive slices of the same region demonstrated co-expression of HCN2 (Fig. 14F). The specificity of the antibodies was verified using sections of cGKII-deficient (Fig. 14G) and HCN2-deficient (Fig. 14H) mice, respectively.

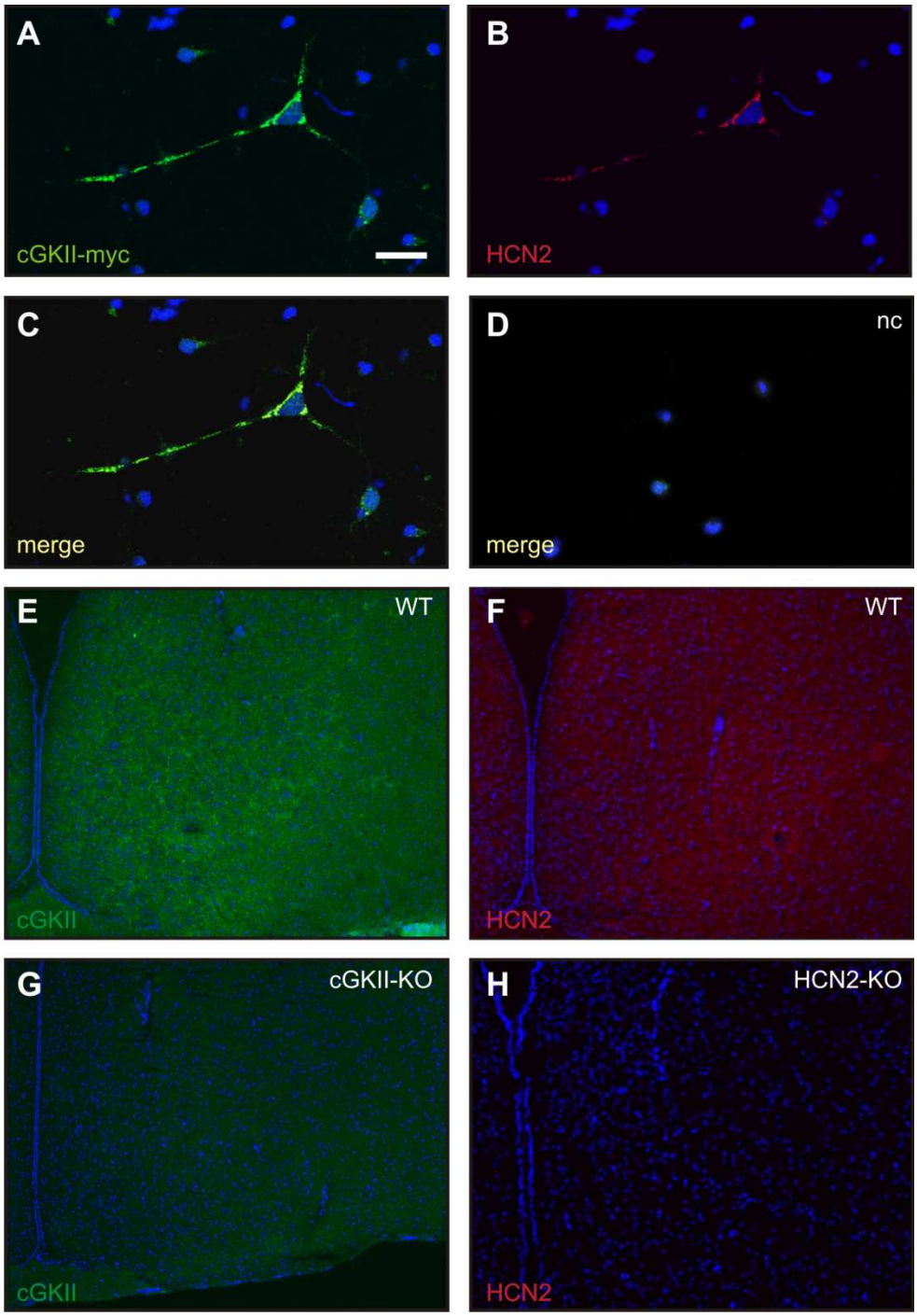

Fig. 14: Co-localization of HCN2 and cGKII in neurons. (A-D) Co-localization in primary neurons. Hippocampal neurons of neonatal mice (E16.5) were co-transduced with lentivirus expressing HCN2 and cGKII-myc, respectively. Neurons were stained with antibodies against myc (A) and HCN2 **(B)** Counter staining was performed with Hoechst dye. **(C)** Merge of **(A)** and **(B)**. **(D)** Negative control (nc). Merge of staining in the absence of primary antibodies. **(E-H)** Immunohistochemical staining of coronal brain slices of the hypothalamic medial preoptic area. Consecutive slices from wild-type mice were stained with anti-cGKII **(E)** or anti-HCN2 **(F)**. The signal was amplified by Cy3 tyramide. Counter stain was performed with Hoechst dye. As negative control, coronal slices of cGKII-KO **(G)** and HCN2-KO mice **(H)** were used. Scale bar corresponds to 100 µm.

3.8 HCN2 is Phosphorylated by cGKII at Position S641

Additionally, it was tested whether HCN2 can be phosphorylated by cGKII. In lysates of HEK293 cells co-expressing HCN2 and cGKII an 100 kDa phosphorylated protein band corresponding to HCN2 appeared after the addition of [γ-^{32}P]-ATP. By contrast, in lysates lacking cGKII the 100 kDa HCN2 was not observed (Fig. 15A). HCN2 contains three serines that are located within a consensus site (K/R-K/R-X-S/T) for phosphorylation by cGKs (S641, S786 and S840; Fig. 16).

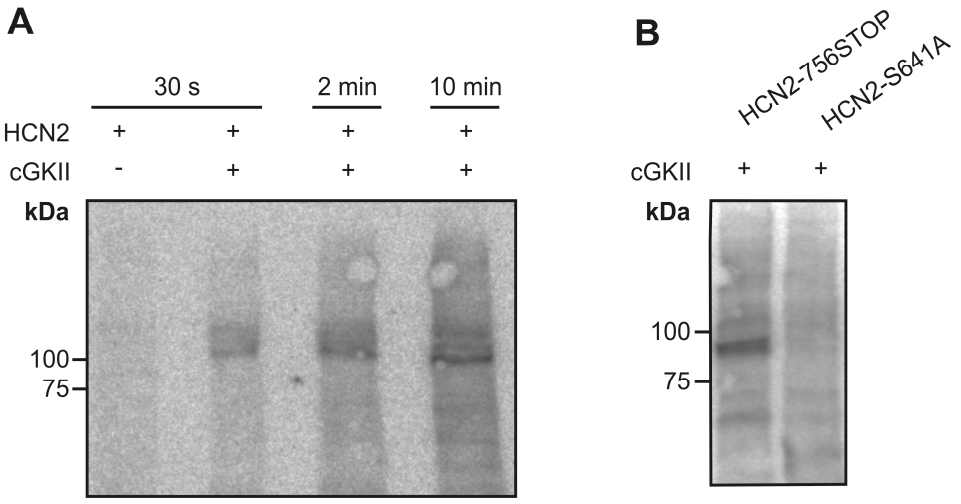

Fig. 15: Phosphorylation of HCN2 by cGKII. (A) *In vitro* phosphorylation of HCN2 by cGKII. Lysates of COS-7 cells expressing HCN2 and cGKII were incubated with [γ-32P]-ATP for the times indicated. After incubation, proteins were separated on SDS page and analyzed by autoradiography. The first lane represents a control reaction with a cell lysate lacking cGKII. **(B)** Phosphorylation assay of a HCN2 mutant lacking S786 and S840 (first lane) and the HCN2-S641A mutant.

Serine 641 is located at the distal end of the α-C helix of the CNBD and is present in all four members of the HCN channel family. By contrast, the two distal consensus sites (S786 and S840) are not conserved throughout the HCN channel family (HCN1 and HCN3 contain no phosphorylation consensus sites at positions equivalent to S786 or S840; HCN4 contains only the consensus site at the position equivalent to S786). A HCN2 truncation mutant lacking the last two serines (HCN2-756STOP) was still efficiently phosphorylated by cGKII (Fig. 15B, left lane). By contrast, a cGKII-dependent phosphorylation of HCN2 was not detectable when S641 was mutated to an alanine (S641A).

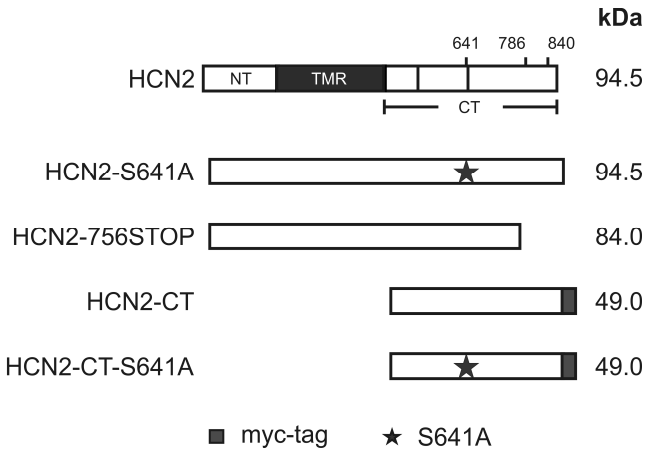

Fig. 16: HCN channel constructs used for phosphorylation studies. The positions of the three putative cGKII phosphorylation sites (S641, S786 and S840) are indicated. The calculated molecular mass is given for each construct.

In order to validate these findings, the binding of C-terminal HCN2 constructs to TiO_2 beads was analyzed (HCN2-CT and HCN2-CT-S641A) (Fig. 17). TiO_2 efficiently binds negatively charged peptides and hence, can be used to determine alterations of the ratio of (highly charged) phosphorylated versus (less charged) non-phosphorylated peptides.

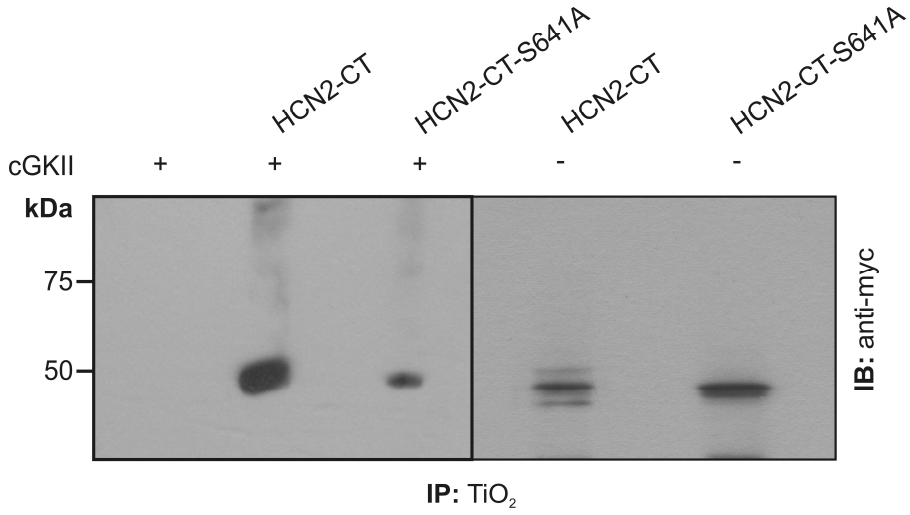

Fig. 17: Pulldown of phosphoproteins by TiO2 beads. Lysates of cells expressing HCN2-CT or HCN2-CT-S641A in the presence or absence of cGKII, respectively, were incubated with TiO_2 beads. Proteins specifically bound to the beads were analyzed with an anti-myc antibody.

After precipitation by TiO_2 and subsequent western blot analysis with anti-myc antibody, a strong 50 kDa band was detected in lysates containing myc-tagged HCN2-CT and cGKII (Fig. 17, second lane). By contrast, only a weak signal was detected for the S641A mutant (Fig. 17, third lane). Bands of

comparable intensity as observed for HCN2-CT-S641A were also obtained in the absences of cGKII indicating that they did not reflect cGKII specific phosphorylation (Fig. 17, last two lanes). Rather, the HCN2 C-terminus may be subject to background phosphorylation by endogenous kinases and/or may be acidic enough in its non-phosphorylated form to bind to some extent to the TiO_2 beads.

3.9 cGKII Shifts the Half Maximal Activation Voltage of HCN2 to More Negative Values

Next, it was tested whether cGKII affects the properties of HCN2-mediated currents. The presence of cGKII had no influence on current densities (current densities at -140 mV: HCN2: -155 ± 24.7 pA/pF, n=15; HCN2/cGKII: -170 ± 43.4 pA/pF, n=7) nor did it influence the activation kinetics of HCN2-mediated currents (τ at -140 mV: HCN2: 293 ± 15.2 ms, n=15; HCN2/cGKII: 309 ± 28.6 ms, n=7).

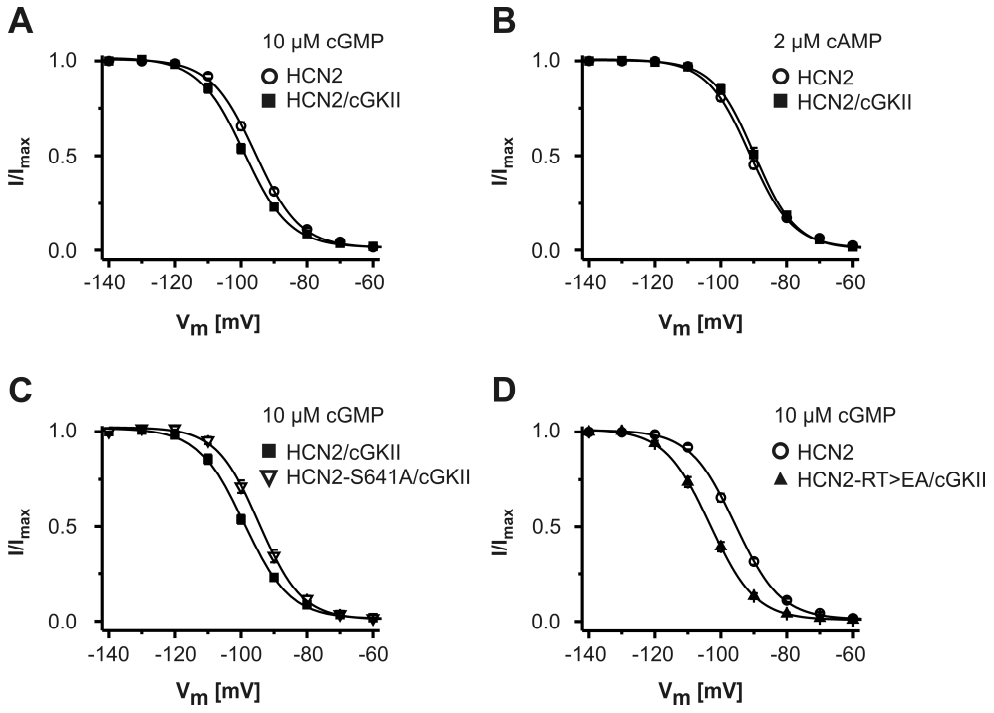

Fig. 18: Regulation of voltage-dependence of HCN2 activation by cGKII. (A) Normalized current-voltage (IV) dependence of HCN2 activation in the presence and absence of cGKII. The voltage-dependence was determined in the presence of 10 µM intracellular cGMP. **(B)** IV curves of HCN2 in the presence or absence of cGKII at 2 µM intracellular cAMP. **(C)** IV curves of HCN2 compared to the IV curve of an HCN2 mutant with functionally impaired cyclic nucleotide binding domain (HCN2 -RT>EA) that was co-expressed with cGKII. Currents were measured in the presence of 10 µM cGMP. **(D)** IV curves determined at 10 µM intracellular cGMP from cells co-expressing cGKII and HCN2 or HCN2-S641A.

However, cGKII led to an about 4 mV hyperpolarizing shift of the voltage-dependence of activation of HCN2 currents ($V_{0.5}$ values at 10 µM cGMP: HCN2: -95.5 ± 0.49 mV, n=16; HCN2/cGKII: -99.3 ± 0.74 mV, n=13) (Fig. 18A). Importantly, the hyperpolarizing shift induced by cGKII was specifically seen in the presence of cGMP, while no shift was observed at 2 µM cAMP (Fig. 18B). It is well known that the $V_{0.5}$ value of HCN2 currents is shifted to more positive values by direct interaction of cGMP with the CNBD (Wahl-Schott and Biel 2009). At 10 µM cGMP which is in the range of the K_a (cGMP) of HCN2 (Ludwig et al. 1998), the voltage shift ($\Delta V_{0.5}$) was about +7.4 mV (Fig. 19, first two columns). In agreement with its inhibitory action, cGKII significantly reduced the $\Delta V_{0.5}$ to about 3 mV (Fig. 19, third and fourth column; $V_{0.5}$ values of HCN2/cGKII at 0 µM cGMP: -102.0 ± 1.25 mV, n=7 and at 10 µM cGMP: -99.3 ± 0.74 mV, n=13).

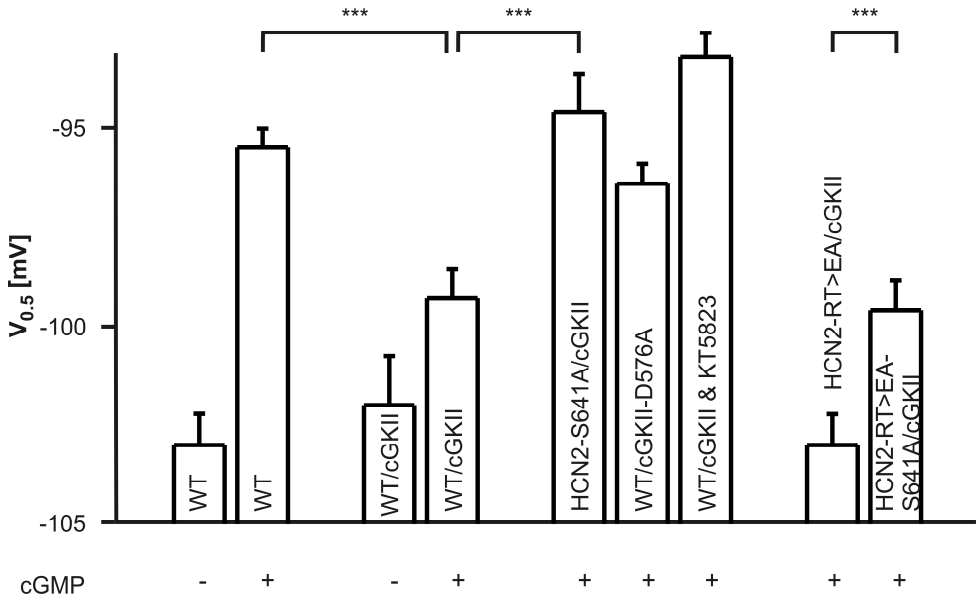

Fig. 19: Comparison of midpoint potentials ($V_{0.5}$) of wild type (WT) and HCN2 mutants (HCN2-S641A, HCN2-RT>EA). Channels were expressed alone or together with either wild type or catalytically inactive GKII (cGKII-D576A). $V_{0.5}$ was determined from the normalized IV curves in the presence (+) or absence (-) of 10 µM cGMP as indicated. In one set of experiments the cGKII was inhibited by the pharmacological blocker KT5823. *** = $p < 0.001$

Additionally, the question was addressed whether phosphorylation at S641 is required for the inhibitory effect of cGKII. In line with this hypothesis, the $V_{0.5}$ value of HCN2-S641A was significantly more positive (-94.6 ± 0.95 mV, n=15) than that of WT HCN2 in the presence of cGKII (Fig. 18C and Fig. 19 fourth and fifth column). Similarly, the inactivation of cGKII by introducing a point mutation in the catalytic domain (cGKII-D576A (Pfeifer et al. 1999)) or by the specific pharmacological blocker

KT5823 abolished the inhibitory cGKII effect on WT HCN2 to a similar extent as the S641A mutation (Fig. 19, sixth and seventh column). Finally, it was of great interest whether the inhibitory effect of cGKII requires binding of cGMP to the CNBD. To this end, a HCN2 mutant was employed (HCN2 -RT>EA) that carries two amino acid replacements in the β7 strand of the CNBD (R591E and T592A) that are known to abolish cGMP binding (Zhou and Siegelbaum 2007). As expected, in the presence of 10 µM cGMP, the $V_{0.5}$ of the HCN2-RT>EA mutant co-expressed with cGKII was much more negative than that of WT HCN2 (Fig. 18D). Importantly, however, introduction of the S641A mutation into the HCN2-RT>EA backbone again lead to a positive shift of $V_{0.5}$ compared to HCN2-RT>EA in the presence of cGKII (Fig. 19, last two column; $\Delta V_{0.5}$ = +3.4 mV; HCN2-RT>EA/cGKII: -103.0 ± 0.77 mV, n=16; HCN2-S641A-RT>EA/cGKII: -99.6 ± 0.76, n=10).

4 Discussion

This study aimed at identifying cellular proteins that regulate HCN channels. Since HCN channels are well understood concerning their functional properties, the question was raised how these channels are modulated within the cellular network. For this purpose, in the first part an Y2H screen of the cDNA library of mouse brain was performed. In this screen, several proteins were identified to bind to the HCN2 C-terminus. The interaction could be verified for all putative candidates in GST-pulldown assays and in Co-IP experiments in HEK 293 cells and immunocytochemistries, respectively. Future experiments will shed light on the functional consequences of these proteins on HCN channels. Especially proteins that are not further characterized up to today are of great interest for future scientific research. Next steps will include a shRNA-based knock-down approach as well as the functional analysis of these proteins *in vivo*.

The major focus of this thesis was to study the interaction of HCN2 and cGKII. It is commonly known that cGMP shifts the $V_{0.5}$ of the HCN2 channels to more positive potentials by direct binding to the CNBD of the HCN2 C-terminus. However, it was unclear whether cGMP can also influence HCN channels via a kinase pathway as it was shown for the PKA in this study. The cGKII could be identified to interact with the HCN2 channel in heterologous expression system as well as in native brain tissue using Co-IP experiments. Furthermore, it could be demonstrated that the CNBD of HCN2 is required for this interaction, either alone or in conjunction with the C-linker.

The cGKII is a membrane bound kinase that belongs to the superfamily of serine/threonine kinases (de Jonge 1981) and has three main domains, an amino terminal (A), a regulatory, and a catalytic (C) domain (Fig. 20). The amino terminus of the cGKII has strong influence on the concentration of cGMP required for the activation of the enzyme. It is noteworthy to mention that the apparent cGMP affinity of HCN2 is about 30 times lower than that reported for cGKII (6 µM vs. 0.2 µM) (Ludwig et al. 1998, Taylor and Uhler 2000). Thus, at very low cGMP concentrations the inhibitory action of cGMP may be dominant while at higher concentrations of cGMP the stimulatory effect may outweight the inhibition imposed by the kinase. Moreover, these data indicate that low micromolar concentrations of cAMP that activate HCN2 currents by binding to the CNBD do not cross-stimulate cGKII and, thus, should not interfere with the cGKII-dependent modulation of HCN2. The regulatory domain consists of two cyclic nucleotide-binding sites whereas the catalytic domain contains the MgATP binding pocket and the protein substrate interaction site (Fig. 20).

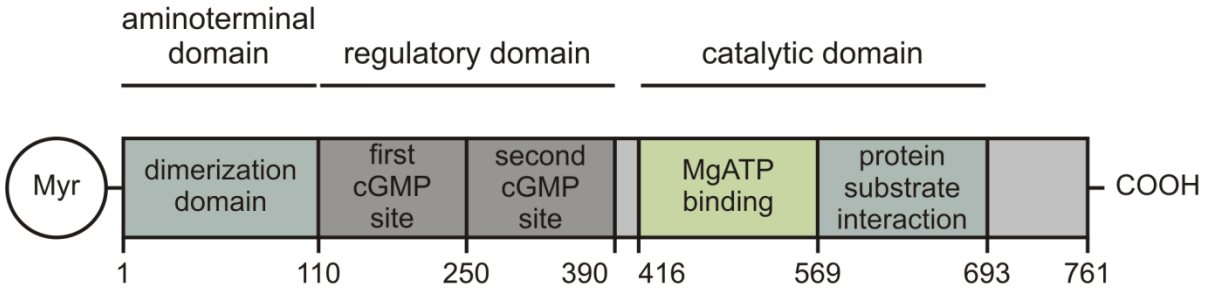

Fig. 20: Cartoon of the cGMP-dependent protein kinase II. A cGKII molecule consists of a regulatory and a catalytic domain. The cGKII forms homodimers that interact over an N-terminal dimerization domain and has two binding sites for cGMP. In the catalytic domain the MgATP binding site and the protein substrate interaction domain are located. The protein is myristylated at aa residue G2. Adapted from Francis and Corbin 1999.

The cGKII is distributed in several brain nuclei, the intestinal mucosa, the adrenal cortex and chondrocytes (Lohmann et al. 1997, de Vente et al. 2001, Werner et al. 2004). Little is known about the substrates of cGKII. Fig. 21 gives an overview of the tissue specific substrates known so far.

A modulatory action of cGKII on other ion channels was only established for the cystic fibrosis transmembrane conductance regulator (CFTR)-Cl^- channel and the AMPA receptor subunit GluR1. In both cases, cGKII was shown to increase the cell surface expression (Serulle et al. 2007). CFTR was also shown to be activated by cGMP/cGKII (French et al. 1995, Golin-Bisello et al. 2005). In this study, the co-expression experiments in HEK293 cells and primary hippocampal neurons do not support an effect of cGKII on HCN2 trafficking and cell surface expression.

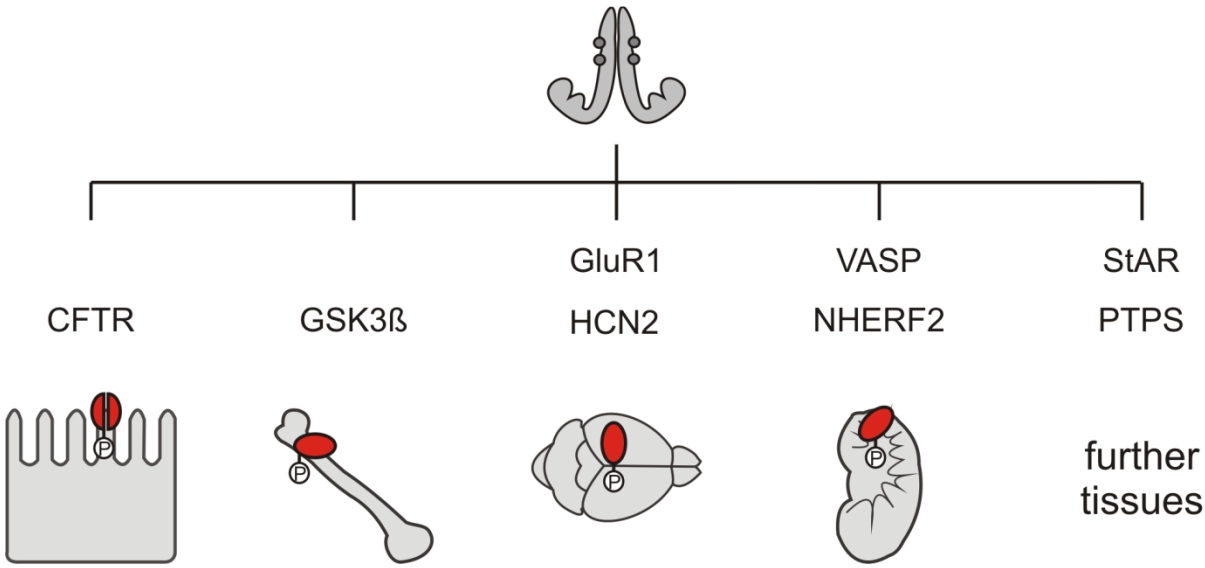

Fig. 21: Interactors of the cGKII. The cGKII phosphorylates the CFTR in the intestinal brush border and the GSK3β in chondrocytes. Furthermore it interacts with GluR1 and HCN2 in brain and with VASP and NHERF2 in kidney, respectively. The cGKII also phosphorylates substrates like StAR and PTPS in other tissues.

During bone growth, the cGKII phosphorylates the glycogen synthase kinase 3β (GSK3β) and inhibits its activity which consequently promotes hypertrophic differentiation of chondrocytes (Kawasaki et al. 2008). Additionally, the cGKII plays an important role in endochondral ossification which could be observed in dwarfism in cGKII KO mice (Pfeifer et al. 1996). In the kidney, VASP is phosphorylated by cGKII in primary mammalian renal tubule epithelial cells. This phosphorylation leads to the rapid retraction of lamellipodia and cell rounding (Lindsay et al. 2007). Recently, it was reported that cGKII plays a role in the aldosterone secretion from the adrenal gland (Spiessberger et al. 2009).

In this study, the HCN2 channel was identified as an additional substrate of cGKII in the brain. The HCN2 channel is phosphorylated at position S641 and this phosphorylation leads to a shift of the $V_{0.5}$ to more hyperpolarized potentials. So far, there are four kinases identified to phosphorylate the HCN channel and subsequently alter the channel kinetics. Whereas the Src kinase accelerates the HCN2 and HCN4 channel kinetics (Zong et al. 2005), the block of the p38 MAPK results in an about 25 mV hyperpolarizing shift in $V_{0.5}$ (Poolos et al. 2006). Other protein kinases, including the protein kinase A might phosphorylate the HCN4 channel at various residues and shift $V_{0.5}$ to about 5 mV to more positive potentials (Liao et al. 2010) (see Fig. 22). It remains to be determined if other kinases may also be able to modulate the function of HCN channels.

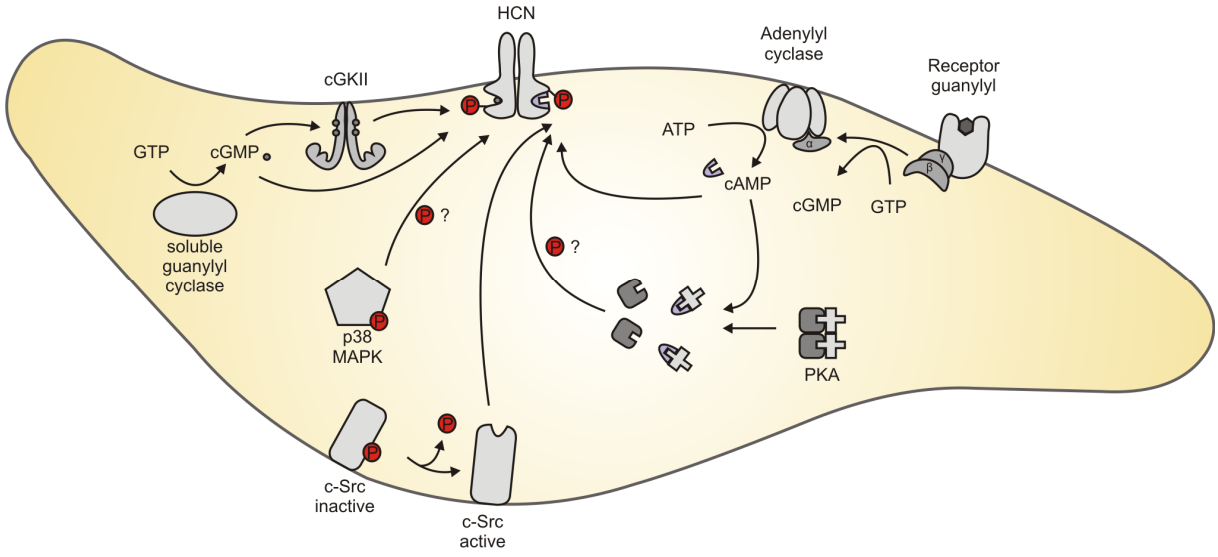

Fig. 22: Modulation of HCN channel activity by protein kinases. Four distinct proteins kinases are known to regulate the HCN channel activity: the c-Src, the p38 MAPK, the PKA and the cGKII.

The PKA was identified to phosphorylate a serine residue inter alia at position 719 (S719) within the HCN4 channel. S719 is a highly conserved amino acid and corresponds to the serine residue at position 641 in HCN2 channels (see appendix 7.5) (Liao et al. 2010). It is unclear, however, whether

S719 is essential for the PKA-mediated effect, because it was shown that at least 13 additional residues are phosphorylated by PKA. It is noteworthy that the results regarding PKA-dependent HCN phosphorylation were obtained using a coupled GST-pulldown assay and subsequent mass spectrometry. Since these experiments were performed in *E.coli* and the work was performed with C-terminal fragments instead of the full length constructs (Liao et al. 2010), these results have to be interpreted with caution and verified in a suitable system.

Table 3: Overview of substrate specificities of the protein kinases interacting with HCN channels.

Kinase	Substrate specificity
MAP kinase [a]	XP(**ST**)XX
Src kinase[b]	EEI**Y**GAFE
	D(ED)(EDG)(IVL)**Y**(GE)E(FI)
cAMP-dependent protein kinase [a]	RX**S**
	RRX**S**
	RXX**S**
	KRXX**S**
cGMP-dependent protein kinase [a]	(KR)X(**ST**)
	(KR)XX(**ST**)
	(KR)(KR)X(**ST**)
	(KR)(KR)XX(**ST**)
	(**ST**)X(KR)

[a] Sequence information based on (Pearson and Kemp 1991), [b] These sequences were determined by the use of peptide libraries (Songyang et al. 1995), and their relevance *in vivo* remains to be determined. X indicates any amino acid; bold characters indicate the site of phosphorylation.

If the phosphorylation pattern of the cAMP-dependent protein kinase is compared to the one of cGKs, it becomes apparent that substrate specificity is not compelling (Table 3). The PKA requires an arginine residue in position two and/or three before the classical phosphorylation site (Tegge et al. 1995), whereas in HCN channels two lysine residues are located at the predicted position (KKNSI). This amino acid sequence represents a classical cGMP phosphorylation site (Table 3). Whether the serine residue can be phosphorylated by both, PKA and cGKII remains to be determined. Thus, phosphorylation is probably a common cellular mechanism to modulate HCN channel activity. An overview of the predicted phosphorylation sites within the HCN channels is shown in the appendix in chapter 7.5. Most substrates of cGMP-dependent protein kinases interact via the substrate interaction site which shows a 71% identity between the cGKII and the cGKI (see appendix 7.6). However, the cGKI was not examined systematically. Owing to the homology of the substrate interaction site, it remains to be determined whether cGKI also interacts with the HCN2 channel subunit.

In this study, for the first time evidence was provided for a bidirectional regulation of the HCN2 channel gating by cGMP (Fig. 23). It has long been known that cGMP, like cAMP, shifts the voltage-dependence of HCN channel activation to more positive values and, thereby, acts as a positive regulator of channel activity (Wahl-Schott and Biel 2009, DiFrancesco 2010). Mechanistically, this regulation is conferred by direct binding of cGMP to the CNBD, which is allosterically coupled to the HCN channel activation gate. Our data indicate that cGMP can also act as gating inhibitor via cGKII-dependent phosphorylation. Here, it was shown that cGKII binds to the C-terminus of HCN2 and phosphorylates this channel at S641. Phosphorylation of S641 shifts the midpoint potential of HCN2 by about 4 mV to more hyperpolarizing values. The effect of cGKII is independent of the capability of the CNBD to bind cGMP since it also occurs in a HCN2 mutant with functionally impaired CNBD.

The exact mechanism underlying the cGKII-mediated inhibition of channel gating remains to be determined. S641 is localized at the C-terminal end of the αC-helix of the CNBD which has been shown to play an important role in HCN channel gating (Zagotta et al. 2003, Xu et al. 2010). One may speculate that the presence of the bulky negatively charged phosphate group could well interfere with the allosteric movement of the proximal C-terminus of HCN2 during channel gating.

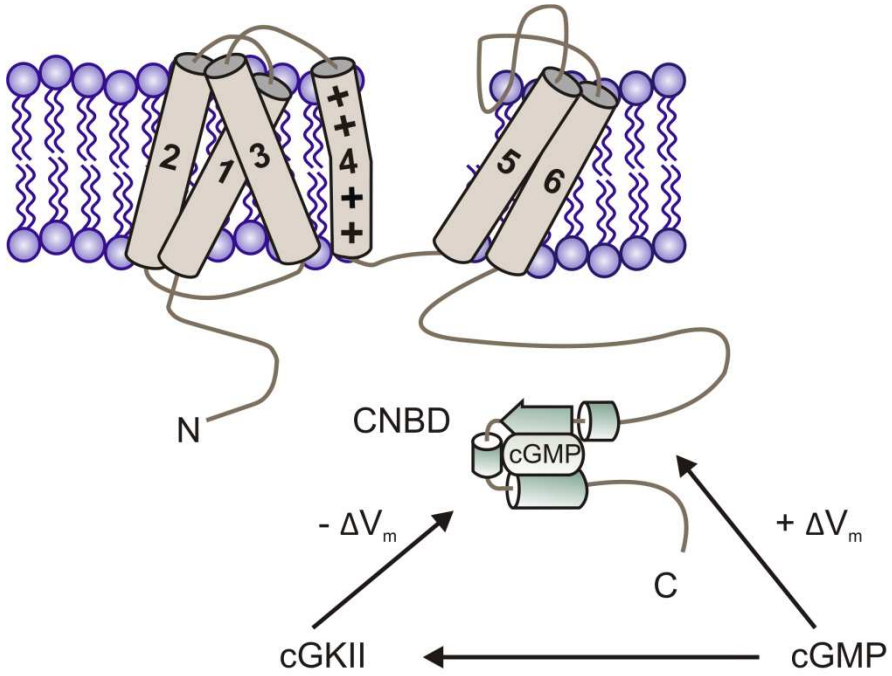

Fig. 23: Model of the bidirectional regulation of HCN2 gating by cGMP. cGMP shifts the voltage-dependence of HCN2 activation to more positive voltage (+ΔV) via direct interaction with the CNBD of HCN2 and induces a hyperpolarizing shift (-ΔV) by activating cGKII that is bound to the channel.

Additionally, this study provides direct experimental evidence for co-localization of HCN2 and cGKII in hypothalamic neurons. Given the widespread distribution of both proteins in brain (Moosmang et al. 1999, Notomi and Shigemoto 2004, Werner et al. 2004), regulation of HCN2 by cGKII could be potentially relevant in many types of neurons. Since S641 is highly conserved within the HCN channel family, this kind of regulation may be a commonality of HCN channels. So far, there are only a few reports on the regulation of I_h by cGMP. Pape et al. showed that NO/cGMP controls oscillatory activity in thalamocortical neurons via direct upregulation of I_h (Pape and Mager 1992) a brain region where the cGKII is located as well at least on mRNA levels using *in situ* hybridizations (El-Husseini et al. 1999, Werner et al. 2004).

In conclusion, this study provides evidence that the voltage-dependence of HCN2 activation is determined by complex interactions of multiple signaling pathways that control the concentration of cGMP and/or cAMP and the activity of cGKII. HCN2 is a key determinant of resting membrane potential in neurons and plays a key role in controlling neuronal excitability (Ludwig et al. 2003). Thus, a cGKII-mediated phosphorylation and change of the value of half-maximal activation of HCN2 in neurons would immediately interfere with neuronal activity because it directly affects the threshold at which HCN2 can be activated.

It is tempting to speculate that in addition to the well established up-regulation of I_h by cAMP and/or cGMP, neurons that express cGKII are also able to down-regulate I_h via the NO/cGMP system by changing the ratio of phosphorylated versus non-phosphorylated HCN2 channels. This “dual modulation by cGMP” may have evolved to allow a tighter control of HCN channel activity, and thus, a better control of the threshold for activation of neurons.

5 Summary

Hyperpolarization-activated cyclic nucleotide-gated channels (HCN) play a crucial role in the regulation of cell excitability and are tightly regulated by interacting proteins as well as low molecular factors. These molecules control functional properties of the channel or modulate the surface expression. In order to find new signaling complexes, an Y2H screen of mouse brain library was performed against the HCN2-CT as bait in a first step. Five distinct mouse brain proteins were identified to form complexes with the HCN2-CT. These genes were cloned and their interaction was verified in GST pulldown assays and co-immunoprecipitations, respectively. Co-localization of the HCN2 subunit and the HCN-interacting proteins could be proofed in immunocytochemistry of COS7 cells.

The major focus of this thesis was to study the interaction between HCN2 and cGKII. Cyclic GMP was shown to facilitate the activation of hyperpolarization-activated cyclic nucleotide-gated (HCN) channels by direct binding to a cyclic nucleotide-binding domain (CNBD) in the C-terminus of the channel protein. Here, it could be shown for the first time that in the HCN2 channel cGMP can also exert an inhibitory effect on gating via cGMP-dependent protein kinase II (cGKII)-mediated phosphorylation. Using co-immunoprecipitation and immunohistochemistry this study demonstrates that cGKII and HCN2 co-localize and interact with each other upon heterologous expression as well as in native brain tissue. The proximal C-terminus of HCN2 was identified as the binding region of cGKII and show that cGKII phosphorylates HCN2 at a specific serine residue (S641) that is localized at the C-terminal end of the CNBD. The cGKII shifts the voltage-dependence of activation to about 4 mV more negative voltages and, hence, counteracts the stimulatory effect of cGMP on gating. Replacement of S641 by an alanine residue, as well as impairing the catalytic activity of cGKII by pharmacological block or by introducing a point mutation into the catalytic domain (D576A) abolishes the inhibitory effect on HCN2 gating. By contrast, the inhibitory effect is preserved in a HCN2 mutant carrying a CNBD deficient for cGMP binding. These data suggest that bidirectional regulation of HCN2 gating by cGMP contributes to cellular fine tuning of HCN channel activity.

Zusammenfassung

HCN Kanäle spielen in der Regulation der Erregbarkeit von Zellen eine entscheidende Rolle und werden durch Interaktionsproteinen sowie niedermolekularen Faktoren engmaschig reguliert. Diese Moleküle kontrollieren die funktionellen Kanaleigenschaften und regulieren die Oberflächenexpression. Um neue Signalkomplexe zu identifizieren, wurde im ersten Teil der Arbeit eine Y2H Analyse durchgeführt. Dabei wurde der C-Terminus des HCN2 Kanals mit einer cDNA-Bibliothek aus dem Mäusehirn abgeglichen. Fünf unterschiedliche Proteine aus dem murinen Gehirn konnten identifiziert werden, die mit dem C-Terminus des HCN2 Kanals Komplexe bilden. Diese Gene wurden subkloniert und die Interaktion konnte in GST-pulldown Versuchen und Ko-Immunopräzipitationen bestätigt werden. Ebenso konnte in Studien in COS7 Zellen eine Ko-Lokalisation der HCN2 Untereinheit mit unterschiedlichen HCN-Interaktionsproteinen nachgewiesen werden.

Der Fokus dieser Dissertation lag auf der Untersuchung der Interaktion vom HCN2 Kanal mit der cGKII. Es ist schon lange bekannt, dass zyklische GMP Moleküle die Aktivierung von HCN Kanälen beschleunigen, indem sie direkt an eine Bindungsdomäne für zyklische Nukleotide (CNBD) im C-Terminus des Kanalproteins binden. In diesem Teil der Arbeit konnte zum ersten Mal gezeigt werden, dass zyklisches GMP auch einen inhibitorischen Effekt auf das Gating von HCN2 Kanälen ausüben kann, indem die cGMP-abhängige Proteinkinase II das Kanalprotein phosphoryliert. Durch Ko-Immunopräzipitationen und Immunohistochemie konnte gezeigt werden, dass der HCN2 Kanal mit der cGKII sowohl in heterologen Expressionssystemen, als auch im nativen Gehirngewebe interagiert und ko-lokalisiert. Der proximale C-Terminus konnte als Interaktionsregion mit der cGKII identifiziert werden und es konnte gezeigt werden, dass die cGKII den HCN2 Kanal an einem bestimmten Serinrest (S641) phosphoryliert wird, der am C-terminalen Ende der CNBD lokalisiert ist. Die cGKII verschiebt die spannungsabhängige Aktivierung des HCN2 Kanals um 4 mV zu negativeren Werten und wirkt so dem stimulierenden Effekt von cGMP auf das Gating entgegen. Der inhibitorische Effekt der cGKII auf das HCN2 Gating konnte sowohl durch den Ersatz des Serinrests durch Alanin an der Position 641, als auch durch pharmakologische Blockade der katalytischen Aktivität der cGKII, als auch durch Einfügen einer Punktmutation in das aktive Zentrum (D576A) aufgehoben werden. Im Gegensatz dazu ist der inhibitorische Effekt in einer CNBD-Mutante aufrecht erhalten, die kein cGMP mehr binden kann. Die Daten dieser Arbeit lassen den Schluss zu, dass die zweigleisige Regulation des HCN2 Gatings durch cGMP einen Beitrag zur zellulären Feinabstimmung leistet.

6 Literature

Ammendola A, Geiselhoringer A, Hofmann F, Schlossmann J. Molecular determinants of the interaction between the inositol 1,4,5-trisphosphate receptor-associated cGMP kinase substrate (IRAG) and cGMP kinase Ibeta. J Biol Chem 276:24153-24159.2001.

Arinsburg SS, Cohen IS, Yu HG. Constitutively active Src tyrosine kinase changes gating of HCN4 channels through direct binding to the channel proteins. J Cardiovasc Pharmacol 47:578-586.2006.

Beaumont V, Zucker RS. Enhancement of synaptic transmission by cyclic AMP modulation of presynaptic Ih channels. Nat Neurosci 3:133-141.2000.

Biel M, Wahl-Schott C, Michalakis S, Zong X. Hyperpolarization-activated cation channels: from genes to function. Physiol Rev 89:847-885.2009.

Biel M, Zong X, Distler M, Bosse E, Klugbauer N, Murakami M, Flockerzi V, Hofmann F. Another member of the cyclic nucleotide-gated channel family, expressed in testis, kidney, and heart. Proc Natl Acad Sci U S A 91:3505-3509.1994.

Biel M, Zong X, Ludwig A, Sautter A, Hofmann F. Molecular cloning and expression of the Modulatory subunit of the cyclic nucleotide-gated cation channel. J Biol Chem 271:6349-6355.1996.

Bradford MM. A rapid and sensitive method for the quantitation of microgram quantities of protein utilizing the principle of protein-dye binding. Anal Biochem 72:248-254.1976.

Brown HF, DiFrancisco D, Noble SJ. Adrenaline action on rabbit sino-atrial node [proceedings]. J Physiol 290:31P-32P.1979.

Brown HF, Giles W, Noble SJ. Membrane currents underlying activity in frog sinus venosus. J Physiol 271:783-816.1977.

Celis JE (1994) Cell biology : a laboratory handbook. San Diego: Academic Press.

Chang F, Cohen IS, DiFrancesco D, Rosen MR, Tromba C. Effects of protein kinase inhibitors on canine Purkinje fibre pacemaker depolarization and the pacemaker current i(f). J Physiol 440:367-384.1991.

Day M, Carr DB, Ulrich S, Ilijic E, Tkatch T, Surmeier DJ. Dendritic excitability of mouse frontal cortex pyramidal neurons is shaped by the interaction among HCN, Kir2, and Kleak channels. J Neurosci 25:8776-8787.2005.

de Jonge HR. Cyclic GMP-dependent protein kinase in intestinal brushborders. Adv Cyclic Nucleotide Res 14:315-333.1981.

de Vente J, Asan E, Gambaryan S, Markerink-van Ittersum M, Axer H, Gallatz K, Lohmann SM, Palkovits M. Localization of cGMP-dependent protein kinase type II in rat brain. Neuroscience 108:27-49.2001.

Decher N, Bundis F, Vajna R, Steinmeyer K. KCNE2 modulates current amplitudes and activation kinetics of HCN4: influence of KCNE family members on HCN4 currents. Pflugers Arch 446:633-640.2003.

Delenda C. Lentiviral vectors: optimization of packaging, transduction and gene expression. J Gene Med 6 Suppl 1:S125-138.2004.

DiFrancesco D. A study of the ionic nature of the pace-maker current in calf Purkinje fibres. J Physiol 314:377-393.1981.

DiFrancesco D. The role of the funny current in pacemaker activity. Circ Res 106:434-446.2010.

DiFrancesco D, Tortora P. Direct activation of cardiac pacemaker channels by intracellular cyclic AMP. Nature 351:145-147.1991.

Dittgen T, Nimmerjahn A, Komai S, Licznerski P, Waters J, Margrie TW, Helmchen F, Denk W, Brecht M, Osten P. Lentivirus-based genetic manipulations of cortical neurons and their optical and electrophysiological monitoring in vivo. Proc Natl Acad Sci U S A 101:18206-18211.2004.

El-Husseini AE, Williams J, Reiner PB, Pelech S, Vincent SR. Localization of the cGMP-dependent protein kinases in relation to nitric oxide synthase in the brain. J Chem Neuroanat 17:45-55.1999.

Fath T, Ke YD, Gunning P, Gotz J, Ittner LM. Primary support cultures of hippocampal and substantia nigra neurons. Nat Protoc 4:78-85.2009.

Frace AM, Maruoka F, Noma A. Control of the hyperpolarization-activated cation current by external anions in rabbit sino-atrial node cells. J Physiol 453:307-318.1992.

Francis SH, Corbin JD. Cyclic nucleotide-dependent protein kinases: intracellular receptors for cAMP and cGMP action. Crit Rev Clin Lab Sci 36:275-328.1999.

French PJ, Bijman J, Edixhoven M, Vaandrager AB, Scholte BJ, Lohmann SM, Nairn AC, de Jonge HR. Isotype-specific activation of cystic fibrosis transmembrane conductance regulator-chloride channels by cGMP-dependent protein kinase II. J Biol Chem 270:26626-26631.1995.

Gamper N, Shapiro MS. Regulation of ion transport proteins by membrane phosphoinositides. Nat Rev Neurosci 8:921-934.2007.

Gauss R, Seifert R, Kaupp UB. Molecular identification of a hyperpolarization-activated channel in sea urchin sperm. Nature 393:583-587.1998.

Golin-Bisello F, Bradbury N, Ameen N. STa and cGMP stimulate CFTR translocation to the surface of villus enterocytes in rat jejunum and is regulated by protein kinase G. Am J Physiol Cell Physiol 289:C708-716.2005.

Graham FL, van der Eb AJ. A new technique for the assay of infectivity of human adenovirus 5 DNA. Virology 52:456-467.1973.

Gravante B, Barbuti A, Milanesi R, Zappi I, Viscomi C, DiFrancesco D. Interaction of the pacemaker channel HCN1 with filamin A. J Biol Chem 279:43847-43853.2004.

Halliwell JV, Adams PR. Voltage-clamp analysis of muscarinic excitation in hippocampal neurons. Brain Res 250:71-92.1982.

Jung S, Bullis JB, Lau IH, Jones TD, Warner LN, Poolos NP. Downregulation of dendritic HCN channel gating in epilepsy is mediated by altered phosphorylation signaling. J Neurosci 30:6678-6688.2010.

Jung S, Jones TD, Lugo JN, Jr., Sheerin AH, Miller JW, D'Ambrosio R, Anderson AE, Poolos NP. Progressive dendritic HCN channelopathy during epileptogenesis in the rat pilocarpine model of epilepsy. J Neurosci 27:13012-13021.2007.

Kawasaki Y, Kugimiya F, Chikuda H, Kamekura S, Ikeda T, Kawamura N, Saito T, Shinoda Y, Higashikawa A, Yano F, Ogasawara T, Ogata N, Hoshi K, Hofmann F, Woodgett JR, Nakamura K, Chung UI, Kawaguchi H. Phosphorylation of GSK-3beta by cGMP-dependent protein kinase II promotes hypertrophic differentiation of murine chondrocytes. J Clin Invest 118:2506-2515.2008.

Kimura K, Kitano J, Nakajima Y, Nakanishi S. Hyperpolarization-activated, cyclic nucleotide-gated HCN2 cation channel forms a protein assembly with multiple neuronal scaffold proteins in distinct modes of protein-protein interaction. Genes Cells 9:631-640.2004.

Lewis AS, Schwartz E, Chan CS, Noam Y, Shin M, Wadman WJ, Surmeier DJ, Baram TZ, Macdonald RL, Chetkovich DM. Alternatively spliced isoforms of TRIP8b differentially control h channel trafficking and function. J Neurosci 29:6250-6265.2009.

Li CH, Zhang Q, Teng B, Mustafa SJ, Huang JY, Yu HG. Src tyrosine kinase alters gating of hyperpolarization-activated HCN4 pacemaker channel through Tyr531. Am J Physiol Cell Physiol 294:C355-362.2008.

Liao Z, Lockhead D, Larson ED, Proenza C. Phosphorylation and modulation of hyperpolarization-activated HCN4 channels by protein kinase A in the mouse sinoatrial node. J Gen Physiol 136:247-258.2010.

Lindsay SL, Ramsey S, Aitchison M, Renne T, Evans TJ. Modulation of lamellipodial structure and dynamics by NO-dependent phosphorylation of VASP Ser239. J Cell Sci 120:3011-3021.2007.

Lohmann SM, Vaandrager AB, Smolenski A, Walter U, De Jonge HR. Distinct and specific functions of cGMP-dependent protein kinases. Trends Biochem Sci 22:307-312.1997.

Ludwig A, Budde T, Stieber J, Moosmang S, Wahl C, Holthoff K, Langebartels A, Wotjak C, Munsch T, Zong X, Feil S, Feil R, Lancel M, Chien KR, Konnerth A, Pape HC, Biel M, Hofmann F. Absence epilepsy and sinus dysrhythmia in mice lacking the pacemaker channel HCN2. EMBO J 22:216-224.2003.

Ludwig A, Zong X, Jeglitsch M, Hofmann F, Biel M. A family of hyperpolarization-activated mammalian cation channels. Nature 393:587-591.1998.

Ludwig A, Zong X, Stieber J, Hullin R, Hofmann F, Biel M. Two pacemaker channels from human heart with profoundly different activation kinetics. EMBO J 18:2323-2329.1999.

Luthi A, McCormick DA. Periodicity of thalamic synchronized oscillations: the role of Ca2+-mediated upregulation of Ih. Neuron 20:553-563.1998.

Magee JC. Dendritic hyperpolarization-activated currents modify the integrative properties of hippocampal CA1 pyramidal neurons. J Neurosci 18:7613-7624.1998.

McCormick DA, Pape HC. Properties of a hyperpolarization-activated cation current and its role in rhythmic oscillation in thalamic relay neurones. J Physiol 431:291-318.1990.

Michels G, Er F, Khan IF, Endres-Becker J, Brandt MC, Gassanov N, Johns DC, Hoppe UC. K+ channel regulator KCR1 suppresses heart rhythm by modulating the pacemaker current If. PLoS One 3:e1511.2008.

Mistrik P, Mader R, Michalakis S, Weidinger M, Pfeifer A, Biel M. The murine HCN3 gene encodes a hyperpolarization-activated cation channel with slow kinetics and unique response to cyclic nucleotides. J Biol Chem 280:27056-27061.2005.

Moosmang S, Biel M, Hofmann F, Ludwig A. Differential distribution of four hyperpolarization-activated cation channels in mouse brain. Biol Chem 380:975-980.1999.

Much B, Wahl-Schott C, Zong X, Schneider A, Baumann L, Moosmang S, Ludwig A, Biel M. Role of subunit heteromerization and N-linked glycosylation in the formation of functional hyperpolarization-activated cyclic nucleotide-gated channels. J Biol Chem 278:43781-43786.2003.

Muller CS, Haupt A, Bildl W, Schindler J, Knaus HG, Meissner M, Rammner B, Striessnig J, Flockerzi V, Fakler B, Schulte U. Quantitative proteomics of the Cav2 channel nano-environments in the mammalian brain. Proc Natl Acad Sci U S A 107:14950-14957.2010.

Munsch T, Pape HC. Modulation of the hyperpolarization-activated cation current of rat thalamic relay neurones by intracellular pH. J Physiol 519 Pt 2:493-504.1999.

Nolan MF, Dudman JT, Dodson PD, Santoro B. HCN1 channels control resting and active integrative properties of stellate cells from layer II of the entorhinal cortex. J Neurosci 27:12440-12451.2007.

Notomi T, Shigemoto R. Immunohistochemical localization of Ih channel subunits, HCN1-4, in the rat brain. J Comp Neurol 471:241-276.2004.

Pape HC, Mager R. Nitric oxide controls oscillatory activity in thalamocortical neurons. Neuron 9:441-448.1992.

Pearson RB, Kemp BE. Protein kinase phosphorylation site sequences and consensus specificity motifs: tabulations. Methods Enzymol 200:62-81.1991.

Pfeifer A, Aszodi A, Seidler U, Ruth P, Hofmann F, Fassler R. Intestinal secretory defects and dwarfism in mice lacking cGMP-dependent protein kinase II. Science 274:2082-2086.1996.

Pfeifer A, Ruth P, Dostmann W, Sausbier M, Klatt P, Hofmann F. Structure and function of cGMP-dependent protein kinases. Rev Physiol Biochem Pharmacol 135:105-149.1999.

Pian P, Bucchi A, Robinson RB, Siegelbaum SA. Regulation of gating and rundown of HCN hyperpolarization-activated channels by exogenous and endogenous PIP2. J Gen Physiol 128:593-604.2006.

Poolos NP, Bullis JB, Roth MK. Modulation of h-channels in hippocampal pyramidal neurons by p38 mitogen-activated protein kinase. J Neurosci 26:7995-8003.2006.

Qu J, Kryukova Y, Potapova IA, Doronin SV, Larsen M, Krishnamurthy G, Cohen IS, Robinson RB. MiRP1 modulates HCN2 channel expression and gating in cardiac myocytes. J Biol Chem 279:43497-43502.2004.

Santoro B, Grant SG, Bartsch D, Kandel ER. Interactive cloning with the SH3 domain of N-src identifies a new brain specific ion channel protein, with homology to eag and cyclic nucleotide-gated channels. Proc Natl Acad Sci U S A 94:14815-14820.1997.

Santoro B, Liu DT, Yao H, Bartsch D, Kandel ER, Siegelbaum SA, Tibbs GR. Identification of a gene encoding a hyperpolarization-activated pacemaker channel of brain. Cell 93:717-729.1998.

Santoro B, Piskorowski RA, Pian P, Hu L, Liu H, Siegelbaum SA. TRIP8b splice variants form a family of auxiliary subunits that regulate gating and trafficking of HCN channels in the brain. Neuron 62:802-813.2009.

Santoro B, Wainger BJ, Siegelbaum SA. Regulation of HCN channel surface expression by a novel C-terminal protein-protein interaction. J Neurosci 24:10750-10762.2004.

Sautter A, Zong X, Hofmann F, Biel M. An isoform of the rod photoreceptor cyclic nucleotide-gated channel beta subunit expressed in olfactory neurons. Proc Natl Acad Sci U S A 95:4696-4701.1998.

Serulle Y, Zhang S, Ninan I, Puzzo D, McCarthy M, Khatri L, Arancio O, Ziff EB. A GluR1-cGKII interaction regulates AMPA receptor trafficking. Neuron 56:670-688.2007.

Songyang Z, Carraway KL, 3rd, Eck MJ, Harrison SC, Feldman RA, Mohammadi M, Schlessinger J, Hubbard SR, Smith DP, Eng C, et al. Catalytic specificity of protein-tyrosine kinases is critical for selective signalling. Nature 373:536-539.1995.

Spiessberger B, Bernhard D, Herrmann S, Feil S, Werner C, Luppa PB, Hofmann F. cGMP-dependent protein kinase II and aldosterone secretion. FEBS J 276:1007-1013.2009.

Stevens DR, Seifert R, Bufe B, Muller F, Kremmer E, Gauss R, Meyerhof W, Kaupp UB, Lindemann B. Hyperpolarization-activated channels HCN1 and HCN4 mediate responses to sour stimuli. Nature 413:631-635.2001.

Stieber J, Stockl G, Herrmann S, Hassfurth B, Hofmann F. Functional expression of the human HCN3 channel. J Biol Chem 280:34635-34643.2005.

Suh BC, Hille B. PIP2 is a necessary cofactor for ion channel function: how and why? Annu Rev Biophys 37:175-195.2008.

Taylor MK, Uhler MD. The amino-terminal cyclic nucleotide binding site of the type II cGMP-dependent protein kinase is essential for full cyclic nucleotide-dependent activation. J Biol Chem 275:28053-28062.2000.

Tegge W, Frank R, Hofmann F, Dostmann WR. Determination of cyclic nucleotide-dependent protein kinase substrate specificity by the use of peptide libraries on cellulose paper. Biochemistry 34:10569-10577.1995.

Tibbs GR, Liu DT, Leypold BG, Siegelbaum SA. A state-independent interaction between ligand and a conserved arginine residue in cyclic nucleotide-gated channels reveals a functional polarity of the cyclic nucleotide binding site. J Biol Chem 273:4497-4505.1998.

Tiscornia G, Singer O, Verma IM. Production and purification of lentiviral vectors. Nat Protoc 1:241-245.2006.

Vargas G, Lucero MT. Modulation by PKA of the hyperpolarization-activated current (Ih) in cultured rat olfactory receptor neurons. J Membr Biol 188:115-125.2002.

Verma IM, Weitzman MD. Gene therapy: twenty-first century medicine. Annu Rev Biochem 74:711-738.2005.

Wahl-Schott C, Baumann L, Zong X, Biel M. An arginine residue in the pore region is a key determinant of chloride dependence in cardiac pacemaker channels. J Biol Chem 280:13694-13700.2005.

Wahl-Schott C, Biel M. HCN channels: structure, cellular regulation and physiological function. Cell Mol Life Sci 66:470-494.2009.

Werner C, Raivich G, Cowen M, Strekalova T, Sillaber I, Buters JT, Spanagel R, Hofmann F. Importance of NO/cGMP signalling via cGMP-dependent protein kinase II for controlling emotionality and neurobehavioural effects of alcohol. Eur J Neurosci 20:3498-3506.2004.

Williams SR, Stuart GJ. Site independence of EPSP time course is mediated by dendritic I(h) in neocortical pyramidal neurons. J Neurophysiol 83:3177-3182.2000.

Wu JY, Cohen IS. Tyrosine kinase inhibition reduces i(f) in rabbit sinoatrial node myocytes. Pflugers Arch 434:509-514.1997.

Xu X, Vysotskaya ZV, Liu Q, Zhou L. Structural basis for the cAMP-dependent gating in human HCN4 channel. J Biol Chem [Epub ahead of print].2010.

Yu H, Chang F, Cohen IS. Pacemaker current i(f) in adult canine cardiac ventricular myocytes. J Physiol 485 (Pt 2):469-483.1995.

Yu H, Wu J, Potapova I, Wymore RT, Holmes B, Zuckerman J, Pan Z, Wang H, Shi W, Robinson RB, El-Maghrabi MR, Benjamin W, Dixon J, McKinnon D, Cohen IS, Wymore R. MinK-related peptide 1: A beta subunit for the HCN ion channel subunit family enhances expression and speeds activation. Circ Res 88:E84-87.2001.

Zagotta WN, Olivier NB, Black KD, Young EC, Olson R, Gouaux E. Structural basis for modulation and agonist specificity of HCN pacemaker channels. Nature 425:200-205.2003.

Zhou L, Siegelbaum SA. Gating of HCN channels by cyclic nucleotides: residue contacts that underlie ligand binding, selectivity, and efficacy. Structure 15:655-670.2007.

Zolles G, Klocker N, Wenzel D, Weisser-Thomas J, Fleischmann BK, Roeper J, Fakler B. Pacemaking by HCN channels requires interaction with phosphoinositides. Neuron 52:1027-1036.2006.

Zolles G, Wenzel D, Bildl W, Schulte U, Hofmann A, Muller CS, Thumfart JO, Vlachos A, Deller T, Pfeifer A, Fleischmann BK, Roeper J, Fakler B, Klocker N. Association with the auxiliary subunit PEX5R/Trip8b controls responsiveness of HCN channels to cAMP and adrenergic stimulation. Neuron 62:814-825.2009.

Zong X, Eckert C, Yuan H, Wahl-Schott C, Abicht H, Fang L, Li R, Mistrik P, Gerstner A, Much B, Baumann L, Michalakis S, Zeng R, Chen Z, Biel M. A novel mechanism of modulation of hyperpolarization-activated cyclic nucleotide-gated channels by Src kinase. J Biol Chem 280:34224-34232.2005.

Zong X, Stieber J, Ludwig A, Hofmann F, Biel M. A single histidine residue determines the pH sensitivity of the pacemaker channel HCN2. J Biol Chem 276:6313-6319.2001.

7 Appendix

7.1 Abbreviations

µg	microgram
µl	microliter
AB	antibody
ADH1	alcohol dehydrogenase-1
Amp^R	ampicillin resistence
BBS	boratesaline buffer
BES	N,N-Bis(2-hydroxyethyl)-2-aminoethanesulfonic acid, N,N-Bis(2-hydroxyethyl) taurine
BES	N-N-Bis(2-hydroxyethyl)-2-aminoethanesulfonic acid
Bp	base pairs
BSA	bovine serum albumine
$CaCl_2$	calcium chloride
cAMP	cyclic adenosine monophosphate
CB	chemiblocker
cDNA	complementary DNA
cGKII	cGMP dependent protein kinase II
cGMP	cyclic guanosine monophosphate
CMV	cytomegalovirus
COS7 cells	cells being **C**V-1 (simian) in **O**rigin and carrying the **S**V40 genetic material
Cre	type I topoisomerase from P1 bacteriophage
DD	Diastolic depolarization
ddH_2O	double deionized water
DEPC	diethyl pyrocarbonate
DMEM	Dulbecco's modified eagle medium
DMSO	dimethylsulfoxide
DNA	deoxyribonucleic acid
dNTP	2'-desoxynucleoside-5'-triphoshate (dATP, dCTP, dGTP, dUTP or dTTP)
DTT	dithiothreitol
E. coli	Escherichia *coli*
EDTA	ethylenediaminetetraacetic acid
EGFP	enhanced green fluorescent protein
env	envelope
FBS	fetal bovine serum
G	gram
GFP	green fluorescent protein
GSK3β	glycogen synthase kinase 3β
GST	glutathione-S-transferase
H	hour
HBSS	Hank's Buffered Salt Solution
HCl	hydrochloric acid
HCN channel	hyperpolarization-activated cyclic nucleotide-gated channel
HEK293 cells	human embryonic kidney cells
HEPES	4-(2-Hydroxyethyl)piperazine-1-ethanesulfonic acid, N-(2-Hydroxyethyl)piperazine-N'-(2-ethanesulfonic acid)
HRP	horseradish peroxidase
IgG	immunoglobulin G

IPTG	isopropyl-β-D-thiogalactopyranosid
IRES	internal ribosome entry site
Kb	kilo base pairs
KCR1	K^+ channel regulator 1
kDa	kilo Dalton
KO	knockout
LB broth	Luria-Bertani broth
LiOAc	lithium acetate
Lox	locus of X-ing over
mA	milliampere
MCS	multiple cloning site
mg	milligram
min	minute
MiRP-1	MinK-related protein 1
Ml	Milliliter
MOPS	3-[N-Morpholino]propanesulfonic acid
mRNA	messenger RNA
$Na_2HPO_4 \cdot 2H_2O$	disodium hydrogen phosphate dihydrate
NaCl	sodium chloride
$NaHCO_3$	sodium bicarbonate
NaOH	sodium hydroxide
NGS	normal goat serum
NP-40	nonyl phenoxylpolyethoxylethanol
OD	optical density
Ori	origin of replication
p38 MAPK	p38 mitogen activated protein kinase
PBS	phosphate buffered saline
PCR	polymerase chain reaction
PEG	polyethylene glycol
Pen/strep	penicillin / streptomycin
PFA	paraformaldehyde
PI	proteinase inhibitor
PIP_2	phosphatidylinositol 4,5-bisphosphate
PKA	proteinkinase A
PKA	cAMP dependent protein kinase
pmol	picomol
PVP	polyvinylpyrrolidone
RNA	ribonucleic acid
RNase	ribonulease
rpm	rotations per minute
RT	reverse transcription
RT-PCR	reverse transcriptase PCR
S	second
SD	synthetic dextrose
SDS	sodium dodecylsulfate
Syn-1	Synapsin-1
Taq	*Thermus aquaticus*
TEMED	N,N,N',N'-Tetramethylethylendiamine
TRIS	*tris*(hydroxymethy1)aminomethane
UF	ultra filtration
-UL	without uracil and leucine
UV	ultra violet

$V_{0.5}$	half maximal activation voltage
V_m	membrane voltage
w/o	without
WT	wildtype
x g	gravitational force
Y2H	yeast two-hybrid

7.2 Primers

7.2.1 HCN2 Genotyping

Primer	Sequenz (5'-3')
HCN2 14F	GGTCCCAGGCACTTCCATCCTTT
HCN2 15bR	GGAAAAATGGCTGCTGAGCTGTCTC
HCN2 16F	CAGCTCCCATTTGCCCTTGTGC

7.2.2 cGKII Genotyping

Primer	Sequenz (5'-3')
AV3R	ATTAAGGGCCAGCTCATTCC
E2FB-AV	GGTGAAGTTTTAGGTGAAACCAAG
AV9R	CTGCTTAATGACGTAGCTGCC

7.2.3 Sequencing

Primer	Sequenz (5'-3')
CMVfor	GGATTTCCAAGTCTCCACC
IRESrev	CAGATGAACTTCAGGGTCAGC
SV40_Rev	GTGGTATGGCTGATTATGATCAG
pcDNA3_For	CTCTGGCTAACTAGAGAAC
pcDNA3_Rev	CAAACAACAGATGGCTGGC

7.2.4 Primers for Cloning

Primer	Sequenz (5'-3')
HCN2BamHIFor	GAGGATCCAAGATTCGTCACGGCGCCAATAC
HCN2SalIRev	AGAGTCGACTCACAAGTTGGAAGAGAGGCGCG
HCN2SalIRev2	AGAGTCGACTCAAACCTTGTGCAGCAAGATGGAG
HCN2SalIRev3	AGAGTCGACTCAGAAGTTGGGGTCTGCATTGGC
HCN2BamHIFor4	GAGGATCCAGGTTCAGCATGATCTCAGCTCAG
HCN2BamHIFo_pQE	AGGATCCGATTCGTCACGGCGCCAATAC
HCN2EcoRIFor	AGAATTCACCGCCATGGATGCGCGCGGGGGCGG
HCN2XbaRev	ATCTAGATCACAGGGACTGGATGAGCGCAGTGGC
HCN2_PFor	TGAGCCGCGCGGCAGCCAGG
HCN2_OL_Rev	TGGTCTTTGTAGTCTCCCAGGGACTGGATGAGCGC
HCN2_OL_For	TCATCCAGTCCCTGGGAGACTACAAAGACCATGAC
LV-RhodProm_PRev	AAGCAGTGGGTTCCCTAGTTAGCC

HCN2_OL_YN155_R	CGCATCCATTCCTGATCCGATATAGACGTTGTGGCTG
HCN2_OL_YN155_F	GTCTATATCGGATCAGGAATGGATGCGCGCGGGGGC
HCN2_OL_YC155_Re	CGCATCCATTCCTGATCCCTTGTACAGCTCGTCCATG
HCN2_OL_YC155_Fo	CTGTACAAGGGATCAGGAATGGATGCGCGCGGGGGC
HCN2BamHI_HAFor	CGGATCCGCCACCATGTACCCATACGATGTTCCAGATTACGCTATGGAT GCGCGCGGGGGCG
HCN2_AgeF	CTGCCCGCTGACTTCCGCCAG
HCN2Term_OL_R	TGGTCTTTGTAGTCTCCCAAGTTGGAAGAGAGGCGCG
HCN2Term_OL_F	CTCTCTTCCAACTTGGGAGACTACAAAGACCATGAC
HCN2_S641E_For	TAGGCAAGAAGAACGAAATCTTGCTGCACAAGG
HCN2_S641E_Rev	TTGTGCAGCAAGATTTCGTTCTTCTTGCCTATGC
HCN2BamHIFor2	GAGGATCCATGGATTCGTCACGGCGCCAATAC
HCN2XbaIRev1	ATCTAGACAAGTTGGAAGAGAGGCGCG
HCN2XbaIRev2	ATCTAGAAACCTTGTGCAGCAAGATGGAG
HCN2XbaIRev3	ATCTAGAGAAGTTGGGGTCTGCATTGGC
HCN2BamHIFor3	GAGGATCCATGGTTCAGCATGATCTCAGCTCAG
mCherry_OL_Rev	CGCATCCATTCCATATGATCCCTTGTACAGCTCGTCCAT
HCN2_OL_For	CTGTACAAGGGATCATATGGAATGGATGCGCGCGGGGGC
HCN2_MluRev	TCCATGAGGAAGAAAGTGTCCG
HCN2_NT_for	AGCTCGGATCCACTAGTAACG
HCN2_NT_XhoI_rev	ACTCGAGGCGCGGCTCACC

7.3 Primary Antibodies

antibody	host	Company	used in	dilution	TSA
HCN2	rb polyclonal	alomone	IHC	1:300	yes
	rb polyclonal	alomone	Western	1:1000	
cGKII	rb polyclonal	Prof. Ruth, Tübingen	IHC	1:100	yes
cGKII Mary EL1	rb polyclonal	Prof. Hofmann, München	Western	1:1000	
Myc	ms monoclonal	Cell Signalling	ICC	1:1000	no
	ms monoclonal	Cell Signalling	Western	1:1000	

7.4 Secondary Antibodies

antibody	host	Company	used in	dilution
α-rb HRP	donkey	Jackson laboratories	IHC	1:1000
α-rb HRP	donkey	GE healthcare	Western	1:1000
α-ms HRP	sheep	GE healthcare	Western	1:2000
Cy2αms	donkey	Jackson laboratories	IHC	1:300
Cy3αrb	donkey	Jackson laboratories	IHC	1:400
Cy3αrat		Jackson laboratories	IHC	1:300

7.5 Phosphorylation sites within the C-terminus of HCN channels

```
mHCN1                                          DSSRRQ YQEKYKQVEQ YMSFHKLPAD  415
mHCN2                                          DSSRRQ YQEKYKQVEQ YMSFHKLPAD  468
mHCN3                                          DSSRRQ YQEKYKQVEQ YMSFHKLPAD  378
hHCN4                                          DSSRRQ YQEKYKQVEQ YMSFHKLPPD  546

mHCN1           MRQKIHDYYE HRYQGKIFDE ENILSELNDP LREEIVNFNC RKLVATMPLF  465
mHCN2           FRQKIHDYYE HRYQGKMFDE DSILGELNGP LREEIVNFNC RKLVASMPLF  518
mHCN3           TRQRIHEYYE HRYQGKMFDE ESILGELSEP LREEIINFTC RGLVAHMPLF  428
hHCN4           TRQRIHDYYE HRYQGKMFDE ESILGELSEP LREEIINFNC RKLVASMPLF  596

mHCN1           ANADPNFVTA MLSKLRFEVF QPGDYIIREG AVGKKMYFIQ HGVAGVITKS  515
mHCN2           ANADPNFVTA MLTKLKFEVF QPGDYIIREG TIGKKMYFIQ HGVVSVLTKG  568
mHCN3           AHADPSFVTA VLTKLRFEVF QPGDLVVREG SVGRKMYFIQ HGLLSVLARG  478
hHCN4           ANADPNFVTS MLTKLRFEVF QPGDYIIREG TIGKKMYFIQ HGVVSVLTKG  646

mHCN1           SKEMKLTDGS YFGEICLLTK GRRTASVRAD TYCRLYSLSV DNFNEVLEEY  565
mHCN2           NKEMKLSDGS YFGEICLLTR GRRTASVRAD TYCRLYSLSV DNFNEVLEEY  618
mHCN3           ARDTRLTDGS YFGEICLLTR GRRTASVRAD TYCRLYSLSV DHFNAVLEEF  528
hHCN4           NKETKLADGS YFGEICLLTR GRRTASVRAD TYCRLYSLSV DNFNEVLEEY  696

mHCN1           PMMRRAFETV AIDRLDRIGK KNSILLQKFQ KDLNTGVFNN QENEILKQIV  615
mHCN2           PMMRRAFETV AIDRLDRIGK KNSILLHKVQ HDLSSGVFNN QENAIIQEIV  668
mHCN3           PMMRRAFETV AMDRLRRIGK KNSILQRK-R SEPSPGSSGG ---VMEQHLV  574
hHCN4           PMMRRAFETV ALDRLDRIGK KNSILLHKVQ HDLNSGVFNY QENEIIQQIV  746

mHCN1           KHDREMVQAI PPINYPQMTA LNCTSSTTTP TSRMRTQSPP VYTATSLSHS  665
mHCN2           KYDREMVQ-- ---------- ------QAEL GQRVGLFPPP PPPQVTSAIA  700
mHCN3           QHDRDMARGV RGL------- --APGTGARL SGKPVLWEPL VHAPLQAAAV  615
hHCN4           QHDREMAHCA HRV------- --QAAASATP TPTPVIWTPL IQAPLQAAAA  787

mHCN1           NLHSPSPSTQ TPQPSAILS- ---------- ---------- ---PCSYTTA  691
mHCN2           TLQQAVAMSF CPQ------- ---------- ---------- ----------  713
mHCN3           TSNVAIALTH QRGP------ ---------- ---------- ---------L  630
hHCN4           TTSVAIALTH HPRLPAAIFR PPPGSGLGNL GAGQTPRHLK RLQSLIPSAL  837

mHCN1           VCSPPIQSPL ATRTFHYASP TASQLSLMQQ PQQ--QLPQS QVQQTQ--TQ  737
mHCN2           -VARPLVGPL ALG------- --SPRLVRRA PPG--PLPPA ASPGPP--AA  749
mHCN3           PLSPDSPATL LAR------- --SARRSAGS PAS--PLVPV RAGPLL--AR  667
hHCN4           GSASPASSPS QVDTPSSSSF HIQQLAGFSA PAGLSPLLPS SSSSPPPGAC  887

mHCN1           TQQQQQQQQQ QQQQQQQQQQ QQQQQQQQQQ QQQQQQ--QQ PQTPGSSTPK  785
mHCN2           SPPAAPSSPR ---------- ---------- ---------A PRTSPYGVPG  770
mHCN3           GPWASTSRLP APPARTL--- ---------- ---------H ASLSRTGRSQ  695
hHCN4           GSPSAPTPSA GVAATTIAGF GHFHKALGGS LSSSDSPLLT PLQPGARSPQ  937

mHCN1           NEVHKSTQAL HNTNLTKEVR PLSASQPS-L PHEVSTLI-- SRPHPTVGES  832
mHCN2           SPATRVGPAL PARRLSRASR PLSASQPS-L PHGVPAPS-- PAASARPASS  817
mHCN3           VSLLGPPPGG GARRLGPRGR PLSASQPS-L PQRATGDG-- SPRRKGSGSE  742
hHCN4           AAQPSPAPPG ARGGLGLPEH FLPPPPSSRS PSSSPGQLGQ PPGELSLGLA  987
```

```
mHCN1           LASIPQPVAA VHSTGLQ--- AGSR-STVPQ RVTLFRQMSS GAIPPNRGVP  878
mHCN2           STPRLGPAPT ARTAAPS--- PDRRDSASPG AASGLDPLDS ARSRLSSNL-  863
mHCN3           RLPPSGLLAK PPGTVQP--- PRSS---VPE PVTPRGPQIS ANM-------  779
hHCN4           TGPLSTPETP PRQPEPPSLV AGASGGASPV GFTPRGGLSP PGHSPGPPRT
1037


mHCN1           PAPPPPAAVQ RESPSVLNTD PDAEKPRFAS NL-------- ---
------ 910
mHCN2           ---------- ---------- ---------- ---------- ----------
mHCN3           ---------- ---------- ---------- ---------- ----------
hHCN4           FPSAPPRASG SHGSLLLPPA SSPPPPQVPQ RRGTPPLTPG RLTQDLKLIS
1087


mHCN1           ---------- ---------- ---------- ---------- ----------
mHCN2           ---------- ---------- ---------- ---------- ----------
mHCN3           ---------- ---------- ---------- ---------- ----------
hHCN4           ASQPALPQDG AQTLRRASPH SSGESMAAFP LFPRAGGGSG GSGSSGGLGP 1137


mHCN1           ---------- ---------- ---------- ---------- ----------
mHCN2           ---------- ---------- ---------- ---------- ----------
mHCN3           ---------- ---------- ---------- ---------- ----------
hHCN4           PGRPYGAIPG QHVTLPRKTS SGSLPPPLSL FGARATSSGG PPLTAGPQRE 1187


mHCN1           ---------- ------
mHCN2           ---------- ------
mHCN3           ---------- ------
hHCN4           PGARPEPVRS KLPSNL                                      1203
```

yellow: phosphorylation by p38 MAP kinase

blue: phosphorylation by src kinase

green: phosphorylation by protein kinase A

red: phosphorylation by cGMP dependent protein kinase

7.6 Alignment of the protein substrate interaction domains of cGKI and cGKII

```
Optimal alignment(Myers-Miller) of DNA sequences
cGKI_protein_substrate_interaction_domain and
cGKII_protein_substrate_interaction_domain

Gap_Open_Penalty=10.0  Gap_Extend_Penalty=5.0

Upper line: cGKI_protein_substrate_interaction_domain, from 1 to 373
Lower line: cGKII_protein_substrate_interaction_domain, from 1 to 375

cGKI_protein_substrate_interaction_domain:cGKII_protein_substrate_interacti
on_domain identity= 71.24%(265/372) gap=1.06%(4/376)
1     CAA..AGGAATCATTTACAGGGACCTCAAGCCGGAGAATCTCATCCTAGATCATCGA.GG
       | ||   |     |     |     |     |     || |  |  |   |||   |
1     CGACTAGGCATCATCTACAGAGACCTGAAGCCAGAGAACTTAATTCTGGAT.GCCGATGG

58    CTATGCCAAACTGGTTGACTTTGGCTTTGCAAAGAAAATAGGATTTGGAAAGAAAACATG
         ||||  ||              |  |  |     |  |  | |    |        |
60    CTACCTTAAGTTGGTTGACTTTGGATTCGCTAAGAAGATTGGCTCTGGACAGAAAACGTG

118   GACTTTTTGTGGGACTCCAGAATATGTAGCCCCAGAGATCATCCTGAACAAAGGCCATGA
         |  |               |     |     |   |    |  |         |
120   GACATTCTGTGGGACTCCAGAGTATGTGGCCCCCGAGGTCATTCTTAACAAAGGACATGA

178   CATTTCAGCTGACTACTGGTCACTAGGAATTCTGATGTATGAGCTTCTGACTGGCAGCCC
       | |||| ||  | |      |  |  |      | |        |  |  |    |
180   CTTCAGTGTGGATTTCTGGTCCCTGGGGATTCTGGTCTATGAGCTCCTAACGGGCAACCC

238   ACCTTTCTCAGGCCCAGATCCAATGAAAACCTACAATATCATACTGCGGGGGATTGACAT
      |  |  |  |  |||   | |     ||          | |  |  |||   |  |  | |
240   TCCCTTTTCTGGGATAGACCAAATGATGACCTACAATTTGATTCTCAAGGGAATCGAGAA

298   GATAGAATTTCCAAAGAAGATTGCAAAAAATGCTGCTAATTTAATTAAAAAACTATGCAG
      |  |  |  |  | ||     ||   ||||||   |||    |  |||| ||  |
300   AATGGATTTCCCCAGAAAGATAACAAGGCGCCCTGAGGATTTGATCCGGAGGCTTTGCAG

358   GGACAACCCATCAGAG
       | ||     |    |
360   GCAAGACCCAACAGAA
```

7.7 Curriculum vitae

Personal Information

Name: Verena Hammelmann

Education

2006-present	PhD at the Department of Pharmacy - Center for Drug Research, Ludwig-Maximilians-Universität München, Germany
2001-2006	Study of Nutritional Science at the Technische Universität München, Germany Master's Degree in Nutritional Science (M.Sc.)
1992-2001	Willstätter Gynasium in Nürnberg, Germany Degree: general qualification for university entrance (allgemeine Hochschulreife)
1988-1992	Primary school in Nürnberg, Germany

Publications

Becirovic E, Nakova K, **Hammelmann V**, Hennel R, Biel M, Michalakis S: The retinitis pigmentosa mutation c.3444+1G>A in CNGB1 results in skipping of exon 32. PLoS One 5:e8969. 2010

Matt L, Michalakis S, Hofmann F, **Hammelmann V**, Ludwig A, Biel M, Kleppisch T: HCN2 channels in local inhibitory interneurons constrain LTP in the hippocampal direct perforant path. Cell Mol Life Sci. 2010

Michalakis S, Zong X, Becirovic E, **Hammelmann V**, Wein T, Wanner T, Biel M: The glutamic acid-rich protein is a gating inhibitor of cyclic nucleotide-gated channels. J Neurosci. (in press) 2010

Hammelmann V, Zong X, Hofmann F, Michalakis S, Biel M: The cGMP-dependent Protein Kinase II is an Inhibitory Modulator of the Hyperpolarization-activated HCN2 Channel. PLoS ONE (under review) 2010

Danksagung

Besonders bedanken möchte ich mich bei Prof. Biel, der immer ein offenes Ohr hatte und stets mit Rat und Tat zur Seite stand sowie die Möglichkeit, diese Arbeit an seinem Lehrstuhl durchführen zu können. In einer Linie damit möchte ich mich bei Stelios bedanken, der stetig meinen Forschergeist heraufbeschwört, auch wenn ich selbst daran einmal zweifle. Vielen Dank für deine konstruktive Kritik und deine Betreuung!

Herzlichen Dank auch an Xiangang für die gute Zusammenarbeit und dafür, dass du unermüdlich den HEK Zellen „lecker Strom“ entlockst und die Ergebnisse mir zur Verfügung gestellt hast.

Den gesamten Arbeitskreis danke ich für die tolle Arbeitsatmosphäre und dafür, dass ich nicht nur Arbeitskollegen, sondern Freunde gefunden habe. Für immer werden mir unsere Mädelsabende, unsere Hüttenwochenenden und die Picknicke am See in Erinnerung bleiben. Danke auch, dass ihr meine Tollpatschigkeit und Verpeiltheit ertragt. Ich hoffe, mit euch noch auf viele erfolgreiche Arbeitstage, erinnernswerte Abende und lustige Ausflüge anstoßen zu können – gerne auch bei „Brot und Frischkäse“.

Allen meinen Freunden abseits der Uni gehört ein Bärenanteil dieser Arbeit. Ihr seid es, die mich ablenken und mir zeigen, dass Probleme zum Lösen da sind. Bei euch komme ich zur Ruhe und tanke Kraft! Danke an meine Nembercher, an Sylvie und besonders an meine Fraunhofer Mädels Brigitte, Caro und Vera. Dicken Knutscha!

Der letzte Abschnitt gehört den wichtigsten Menschen in meinem Leben: Meiner Mama, meinem Papa, meiner Schwester Sarah und meinem „gefühlten“ Bruder Momo. Ohne eure Liebe und Unterstützung wäre das alles nicht möglich gewesen. Ihr wisst gar nicht, wie viel ihr mir bedeutet!